TÉCNICO LISBOA

Relationship between surface and subsurface soil moisture content for various land uses

Peizo Rachel Cheng

Thesis to obtain the Master of Science Degree in

Environmental Engineering

Supervisors: Prof. Doutor Wim Bastiaanssen
Prof. Doutor Rodrigo Proença de Oliveira

Examination Committee

Chairperson: Prof. Doutor Luís Filipe Tavares Ribeiro
Supervisor: Prof. Doutor Rodrigo Proença de Oliveira
Members of the Committee: Doutor G. J. Roerink,
Doutora Maria Teresa Condesso de Melo,
Prof. Doutor Rodrigo Proença de Oliveira

August 2017

Relationship between surface and subsurface soil moisture content for various land uses

Master of Science Thesis
by

Peizo Rachel Cheng

Supervisors
Wim Bastiaanssen
Rodrigo Proença de Oliveira

Examination committee
Luís Filipe Tavares Ribeiro
G. J. Roerink
Maria Teresa Condesso de Melo
Rodrigo Proença de Oliveira

This thesis is submitted in partial fulfilment of the requirements for the academic degree of

Master of Science in Water Science and Engineering
UNESCO-IHE Institute for Water Education, Delft, the Netherlands

Master of Science in Environmental Engineering
Instituto Superior Técnico, Universidade de Lisboa, Portugal

Master of Science in Hydro Science and Engineering
Technische Universität Dresden, Germany

MSc research host institution
UNESCO-IHE, Delft, the Netherlands

September 2017

Acknowledgements

I would like to humbly acknowledge Dr. Wim Bastiaanssen and Dr. Gonzalo Espinoza for their continued willingness to support my work. I equally thank my family, friends, and the Water Accounting Team for all their positive words of encouragement over these past few months.

The original version of this work has been reformatted for submission to the Instituto Superior Técnico, Universidade de Lisboa, Portugal and is based upon formatting provided graciously by my colleague Raghwendra Narayan Shandilya. My warmest appreciation is sent to my Mr. Shandilya for the guidance and true friendship he has provided over these past two years.

Thank you.

Resumo

A capacidade da deteção remota para detetar parâmetros superficiais em resoluções temporais e espaciais adequadas abre perspetivas sobre a possibilidade de estimar a humidade subsuperficial baseada nos atributos da medidos à superfície. Este trabalho investiga a possibilidade de estimar a humidade ao longo de um perfil de solo e as relações físicas e ambientais que a influenciam no estado de Nebrasca (Estados Unidos) que é maioritariamente agrícola. A humidade na zona das raízes é estimada a partir de cinco modelos baseados na fração evaporativa, humidade superficial, temperatura e índices de vegetação. Com base em 45 estações que representam diferentes tipos de solo existentes em todo o estado, é realizada uma avaliação do índice de humidade do algoritmo de estimação da evapotranspiração ETLook, calculado pelo espectómetro ASCAT. São também estimados três outros índices de humidade do solo na zona das raízes baseados em modelos que relacionam a humidade do solo e a fracção evaporativa. A profundidade da zona do solo é calculada através da comparação do perfil de humidade do solo com o calculado pelo modelo SWAT para três locais.

Os três casos de estudos fornecem uma base para avaliar o desempenho dos modelos em várias situações de uso da terra e de utilização da água, e que podem ser utilizados para estimar a humidade da zona radicular por monitorização remotos.

Palavras-chave: Humidade zona de raízes, SWAP, ASCAT SWI, ETLook, Fração evaporativa

Abstract

The ability of remote sensing to detect surface parameters at temporally and spatially consumable resolutions provides a potential avenue to estimate subsurface moisture based upon surface attributes. This paper explores the estimation and depth of moisture at the near surface and within the soil profile along with the physical and environmental relationships which influence the two for the agriculturally dominated state of Nebraska, United States. Root zone moisture content is estimated from five models based upon the evaporative fraction, surface moisture, temperature, and vegetation indices. A state-wide evaluation of ASCAT surface moisture index for ET Look root zone moisture estimation consisting of 45 stations representing various land types is performed. In addition to the ET Look model, three additional sets of root zone moisture estimations based upon a model relating soil moisture and evaporative fraction are included in this study, along with an adjusted model. Root zone depth is approximated by comparing subsurface moisture estimations to moisture profile simulations from the agro-hydrology model SWAP for three case study locations. The three case studies provide a basis for evaluating the models over varying land cover and water management schemes to resolve the hurdles which deter remotely sensed root zone moisture estimation from near surface factors.

Keywords: *Root zone soil moisture, SWAP, ASCAT SWI, ETLook, Evaporative fraction*

Table of Contents

List of Figures

List of Tables

CHAPTER

1

Introduction

Availability of fresh water resources on volcanic islands located in semiarid climatic regions are limited and extremely susceptible to climate changes and management practices. Water in rivers and streams are often confined to the high relief areas of the islands and/ or to short periods after the heavy rainfall events, which occasionally occur during the wet season. Shortage of surface water and less rainfall leaves groundwater resources are usually the principal source of fresh water for local population and agriculture use. However, due to the trivial water scarcity problems that affect these regions, the attention is placed on groundwater quantity rather than quality and groundwater resources face an increasing risk of contamination.

Salinization of groundwater is one of most prominent cause of groundwater contamination on volcanic islands, which may result from natural rock-water interaction processes (cation exchange, dissolution, surface complexation) between circulating groundwaters and volcanic materials that are enriched in several geochemical elements (Cl, Na, Si, As, F); or, from seawater intrusion due to non-sustainable groundwater abstraction. High evaporation rate may also contribute for salt accumulation in areas with shallow water levels.

1.1 Study Area

Porto Santo is a volcanic island part of the Madeira archipelago that is situated in the Atlantic Ocean, west of southern Europe and northern Africa (Figure 1). It is a small island (42.2 km^2) extending between 32º 59' and 33º 07' N parallels of latitude and 16º 16' and 16º 24' W meridians of longitude and together with the volcanic archipelagos of Madeira, Azores, Canary and Cape Verde is part of the Macaronesia biogeographical region. It is quite a flat island but characterized by two distinct regions, the northeast part where some of the highest peaks are located is rugged, while the southwest corresponds to a low lying coastal plain with a nine-kilometer-long white sand beach. The island has a semi-arid climate and average annual rainfall is less than 500 mm, occurring often as short heavy events that may produce flash floods and strong landscape erosion (locally called 'badlands'). The soils for agriculture are sandy and poor in nutrients and the island has very scarce freshwater resources relying mostly on groundwater for irrigation and seawater desalination for public water supply.

Porto Santo is inhabited by 5000 year-long residents of which the majority lives in the capital (Vila Baleira) but the population significantly increases during the summer months. Tourism has given Porto Santo an economic dynamism that has been growing year by year. The warm climate and sea, the

quietness and remoteness of the island, the therapeutic qualities of its sands that are proved to help treat skin, orthopedic and rheumatic problems are bringing many tourists to the island and contributing decisively to the island's economic and touristic expansion. Nowadays, the population of tourists and part-time second house residents fluctuates between 500 in the winter months and 15,000 in the summertime, exceeding three times the resident population and increasing significantly the pressure on local water resources and services.

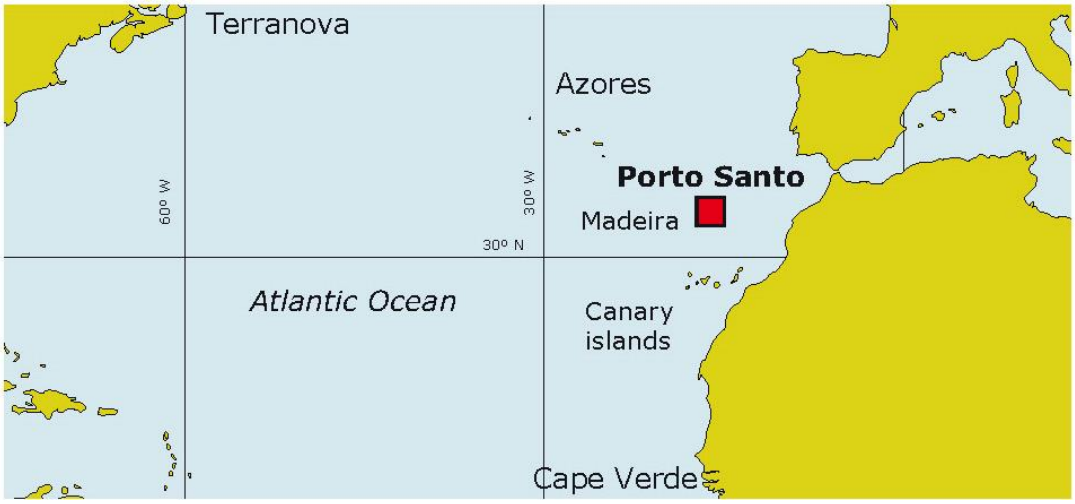

Figure 1. Location of Porto Santo island (adapted from Silva, 2003).

Porto Santo has very limited availability of water resources due to both geological (predominant low permeability volcanic formations), geomorphological (size and low altitude) and climatic conditions (meagre rainfall and high evapotranspiration rates). Most surface water circulation occurs in small streams ('*ribeiros*' in Portuguese) and are in close relation to springs or mines that tap groundwater levels. Groundwater resources are limited in general to the principal sedimentary formations in the central part of the island tapped by shallow wells (< 30 m deep), as most of the volcanic formations are low permeability and just occasionally have perched aquifer formations that feed some of the springs and fountains around the island. Moreover, groundwater resources in Porto Santo are strongly constrained for human consumption and irrigation by their high salinity that can occur naturally or result from human activities.

1.2 Previous investigations

From the hydrogeological point of view there have been very few investigations in Porto Santo. Lobo Ferreira *et al*., (1981) wrote a techinical report on the water resources of Porto Santo island, Ferreira & Neiva, (1996) are the authors of the geological and hydrogeological maps of the island and Duarte, (1988) presented a conference paper about prospection of groundwater resources in the Madeira archipelago. Condesso de Melo *et al.*, (2008) carried out the first detailed investigation about the groundwater quality and source of groundwater salinity on the basis of major geochemical patterns, ionic ratios and stable isotopic measurements. Antunes *et al.*, (2008) authored one the few selected researches on the island which deals with soil physical and chemical characteristics . Soil samples from nine different locations ranging in altitude of 20 meters above mean sea level to 330 meters above sea

level were collected for the measurement of electrical conductivity, pH, water and organic matter content measurement. Almost all sampling sites were identified as alkaline in nature and the highest electrical conductivty value of 558 µS/cm was recorded during summer months.

Most important research in the Porto Santo island have been concentrated on the geological, geomorphological and ethnopharmacological aspects. Morais (1943) presented the first study of Porto Santo geology, Schmincke & Weibel (1972) and Schmincke & Staudigel (1976) carried out a preliminary chemical study of Porto Santo rocks. Fèraud *et al*., (1981) reported new K-Ar ages, chemical analysis and magnetic data of Porto Santo island, Ferreira *et al.*, (1988) have studied the geological and geochronological sequence using an extensive programme of K-Ar dating. The lithological succession of the base complex which consist of basanitic hyaloclastites, tuffites, pillow basalt and reef limestones has been identified in the study. The K-Ar dating established the age of visible section between 18.8 to 13.5 m.y. Rivera & Obon (1995) has studied about the peculiarities of the medicinal flora from Porto Santo and Madeira. A total of 259 species of medicinal flora has been identified from both islands and discussed about the importance of culture and biogeographic features of the island in making it center of medicinal plant diversity. Cachão *et al*., (1998) carried out a preliminary study using of the biostratigraphy and palaeoenvironmental interpretation of the Neogene in Porto Santo and later (Cachão, *et al*., 2003) investigated the island geological evolution and its palaeoenvironments. Schmidt & Schmincke (2002) investigated the rise of the Porto Santo island. The study focussed on emergence of the shallow water seamount of Porto Santo, and identified numerous dynamic processes that contributed to growth and stabilization of the edifice in its present form. The authors showed that the processes included submarine and subaerial phreatomagmatic and pyroclastic explosions, submarine explosive imploding, and quench fragmentation of extrusive domes, as well as submarine and subaerial effusive activity. Silva (2002,2003) studied in detail the origin, genesis and evolution of the sands in Porto Santo. Cordeiro *et al.*, (2010) has discussed the surface properties of the local bentonite clay found on the island and their potential value, achieved through their incorporation in products for dermopharmacy and dermocosmetics. Ribeiro & Ramalho, (2010) wrote a detailed geological tour of the Archipelago of Madeira which includes details on Porto Santo and Mata *et al.*, (2013) presented another very good and detailed geological synthesis of the Porto Santo island.

1.3 Scope and objectives

Numerous hypotheses can be related to the development of salinity in the semi-arid landscape of the Porto Santo island (Figure 2). High evaporation, remnant sea water entrapped in the sedimentary sediments at the time of their deposition, airborne oceanic aerosols (cyclic salts) transported inland into basins by rainfall or a combination of rock weathering and marine aerosol accession are the probable causes of salinity in the semi-arid regions has been discussed so far (Bonython, 1956; Wopfner & Twidale, 1967; Chivas *et al.*, 1991; Mazor & George, 1992; Custodio, 1993).

Rock weathering involves natural mixing between water and aquifer materials that give rise to a wide diversity in the mineral character of groundwater. The minerals prove to be very much decisive in imparting intrinsic properties such as hardness and softness, salinity and even bitterness and

sweetness. Groundwater quality evolves quickly as it advances through the subsurface pathways within the soil and the vadose zone, and thence to the saturated zone of the aquifer. The mineral assemblage of the host rock, the relative abundance of individual minerals, solubility, crystallinity and purity are major governing factors of the water quality. However, even a less dominant mineral which dissolve rapidly, such as calcite (in veins or as a cement) may dominate the water quality even in some silicate-dominated lithologies (Cook, et al., 1991).

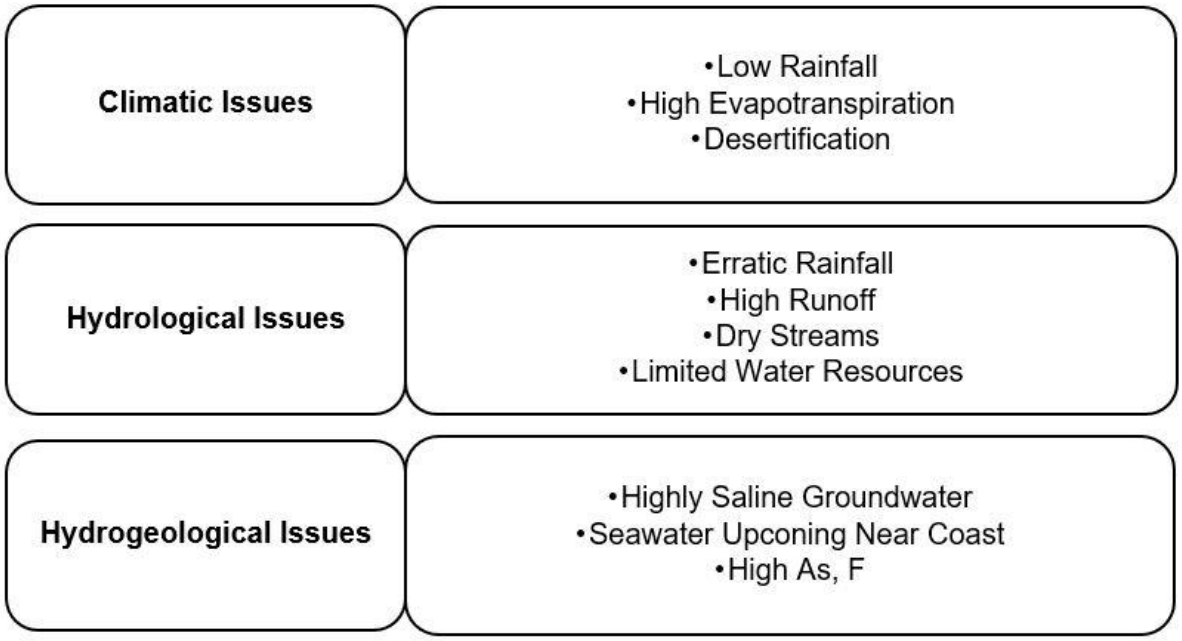

Figure 2 Summary of the main issues concerning groundwater quantity and quality in the Porto Santo island

Accumulation of salt is another reason for inland groundwater salinization. Deficit in water budget caused by high evaporation rates and low precipitation in semi-arid and arid regions is very often combined with the severe contamination of the available water resources by dissolved inorganic salts to an extent that their utilization for any purposes is impossible. In undrained or poorly managed basins, the salts get concentrated either on the surface or in soil profiles, which serves as a potential source of dissolved materials that can be carried down to groundwater following a rainy or water level fluctuation phenomenon. Residual brines and leachates are another source that increase the groundwater salinity after encountering the percolating water (Datta *et al.,* 1996; Gilfedder *et al.,* 2000). The formation of saline water often results from salt leaching, when groundwater circulates along the evaporites bearing soils or rocks (Cooper, 2002; Simpson & Herczeg, 1991).

Primary salinization of groundwater also occurs through sea salt aerosols (SSA), which are produced via the bursting of bubbles at the air-sea interface during low to medium speed winds. SSA are geochemically important for the transport of several trace species between ocean and the atmosphere (Weisel *et al.*, 1984; Savoie & Prospero, 1982). The production and transport of SSA is generally thought to be directly related to wind speed, thus those regions of the world ocean that experience relatively high wind speeds are also areas of high atmospheric sea-salt production (Blanchard, 1985).

Rainfalls wash out the accumulated SSA, which can reach groundwater determining consequently an increase of salinization. Number of studies pertaining to quantify the volumes (Erickson & Duce, 1988; Gong *et al.*, 2002) and the size of aerosol particles depending on wind velocity in laboratory experiments (Mårtensson *et al.*, 2003; Fuentes *et al.,* 2010) have already been carried out.

The increasing demand of fresh water resources in Porto Santo and the opportunity to include groundwater resources in the water management practices to minimize costs of water supply for irrigation and touristic activities, requires a detailed study of the groundwater quality and quantity in the island. The study of groundwater quality origin and evolution is the main objective of this research. Other objectives of the present work include:

- Identification of groundwater types based on aquifer lithology
- Major geochemical patterns in the groundwater evolution
- Groundwater salinity source identification
- Minor and trace elements identification
- Groundwater recharge estimation
- Recommendation for improving water conservation practice on the island to face global change.

The methodology adapted to carry out the study followed several steps summarised in the flow chart illustrated in Figure 3. The study has been initiated with the identification of the main research goal, which is to provide a new insight that may be used for both interpretative and descriptive purposes about the origin of salinity in the groundwater of Porto Santo. The study may have its significance in wake of changing climate and the measures to mitigate the effects.

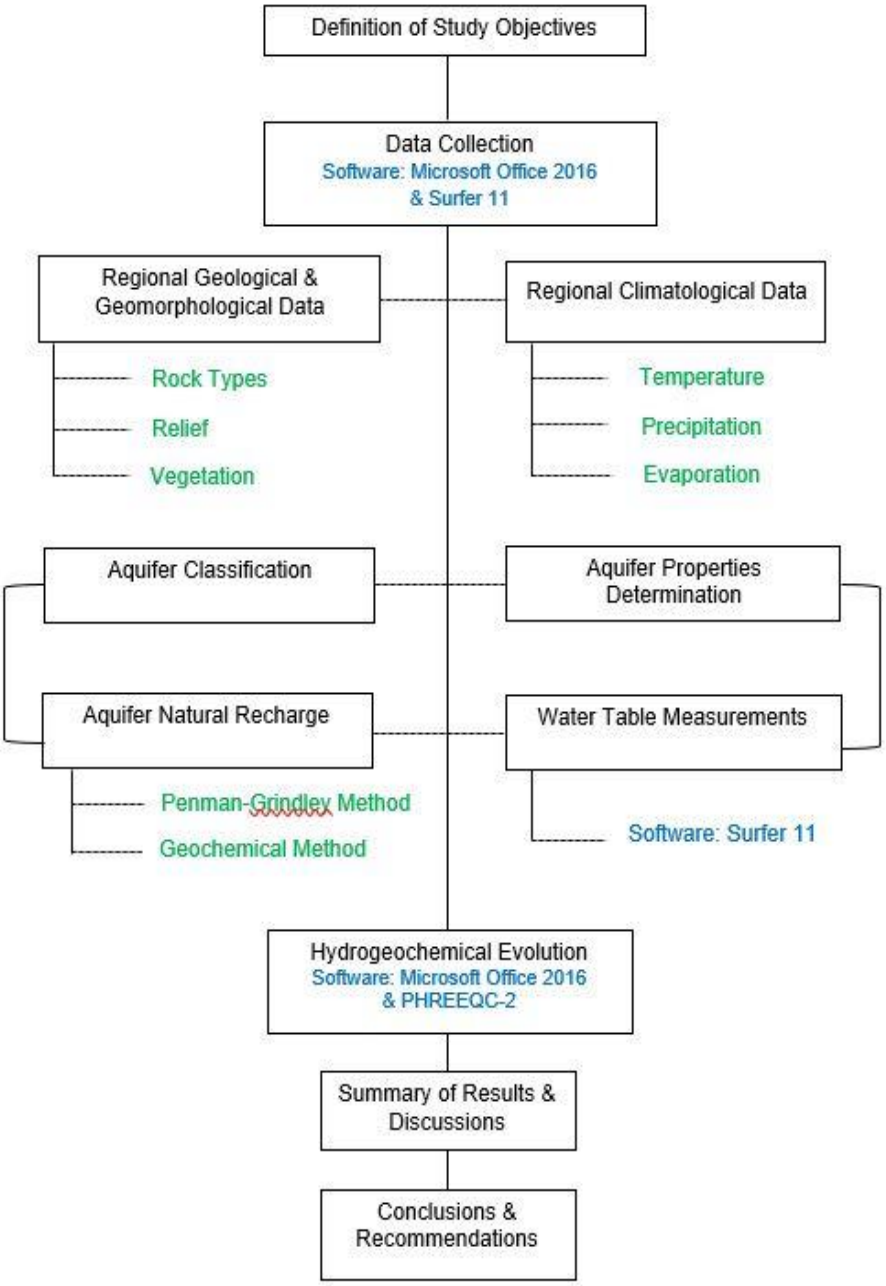

Figure 3 Flow chart describing methodology followed during the study

CHAPTER

2

Geology, Geomorphology and Hydrogeology

The island of Porto Santo is deep seated in the ocean floor, which was generated by the separation of the African and American tectonic plates known as Mid-Atlantic Rift (Ribeiro & Ramalho, 2010) (Figure 4). The island, for that reason, is typical example of oceanic ridge basalt volcanism. Emplacement of the volcanic rocks on the surface differs in age. Trachyte from the submarine mount has been dated by several workers and K-Ar chronology dates varies from 12.3±0.4 (Feraud, *et al*., 1981) to 16.4 m. y (Macedo, *et al*., 1974). Majority of exposed eruption in Porto Santo is expected to have occurred in mid Miocene approximately 12.5 to 13.8 m. y., and thus the basement rocks are found synchronous in age with Gran Canaria whose sub aerial mount dates to 13.5 to 14.0 m. y (McDougall & Schmincke, 1976). Varying dates proposed by authors led to no specific conclusion about submarine volcanism of Porto Santo rather gave a general statement about underwater orogeny process.

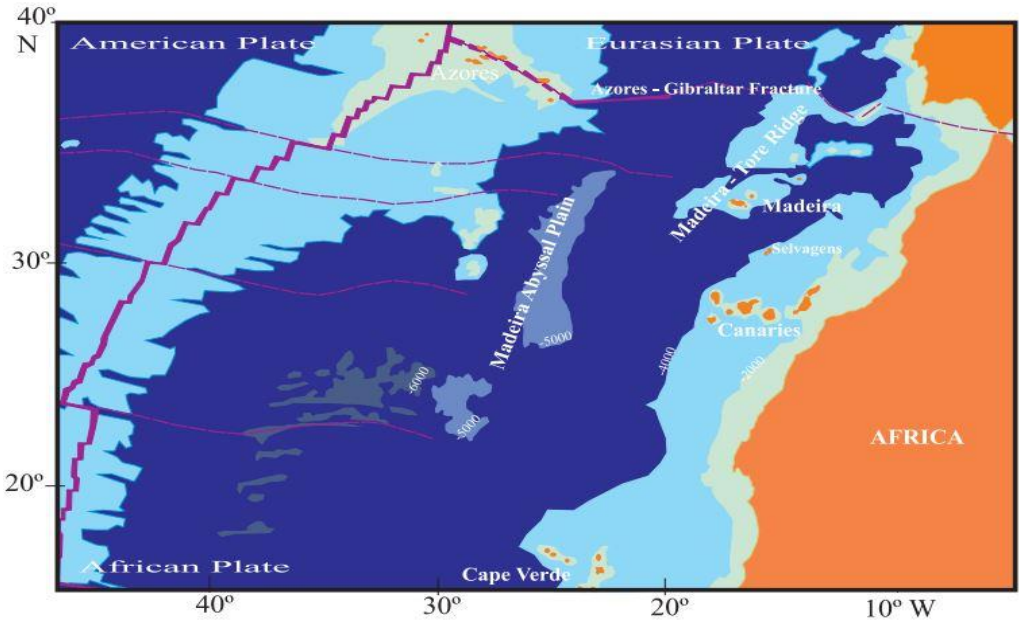

Figure 4 Location of the Archipelago of Madeira within the major geological units of the submersed part of the African plate. In red: The Mid-Atlantic Ridge and major active faults. The ocean depths are represented by: green (0 – 2,000m), light blue (2,000 – 4,000m), dark blue (4,000 – 6,000m) and dark gray (more than 6,000m depth) [from (Ribeiro & Ramalho, 2010)].

The oldest geochronological ages, known so far, do not exceed the 5.2 million years (lower Pliocene) on Madeira isalnd. Thus, despite some uncertainties regarding the ages of these islands, all authors acknowledge that the island of Porto Santo preceded the island of Madeira by several million years and

a conscientious regarding migration of the volcanism towards SSW, from the island of Porto Santo to the island of Madeira, between the Miocene and the Pliocene.

Various theories have been put forward regarding source and depth of hotstop generating the magma, and the height of water column above the volcanic rocks emplacement on ocean floor. The geochemical and isotopic study of the alkaline sequence has been done by Mata *et al*., 1998 to know the depth at which magma originated. Mata *et al.,* (1998) concluded that the magma that has formed the island of Porto Santo originated from hotstop plume formed within asthenosphere at depth of about 125 km.

Study of fossils assemblage, conglomerate sequence, vesicularity of juvenile particles and volatile content of fresh volcanic glass has the potential to give conclusive evidence about the water depth of submarine volcanism. Based on vesicles in juvenile particles from the lower and upper scoria cones, Fisher & Schmincke (1984) have concluded shallow water depth of submarine volcanic and depositions. Presence of conglomerate capping near the upper scoria cone indicates shoreline depositional environment at water depth of not more than a few tens of meter (Schmidt & Schmincke, 2002). Sulphur concentration in the sideromelane particles from the scoria cone conglomerates ranges between 200 to 600 ppm (Schmidt, 2000), indicating shallow water to subaerial eruptions (Moore & Clague, 1992). Based on Schmidt & Schmincke (2002), hermatypic corals are the the main constituent of the small patch reef embedded in the upper scoria cone, which points to growth with in the photic zone.

2.1 Geology

The geological formation of Porto Santo consists of mainly of two rock types: igneous rocks, mainly basalts, directly linked to the volcanic origin of the island itself, and sedimentary rocks (Figure 5).

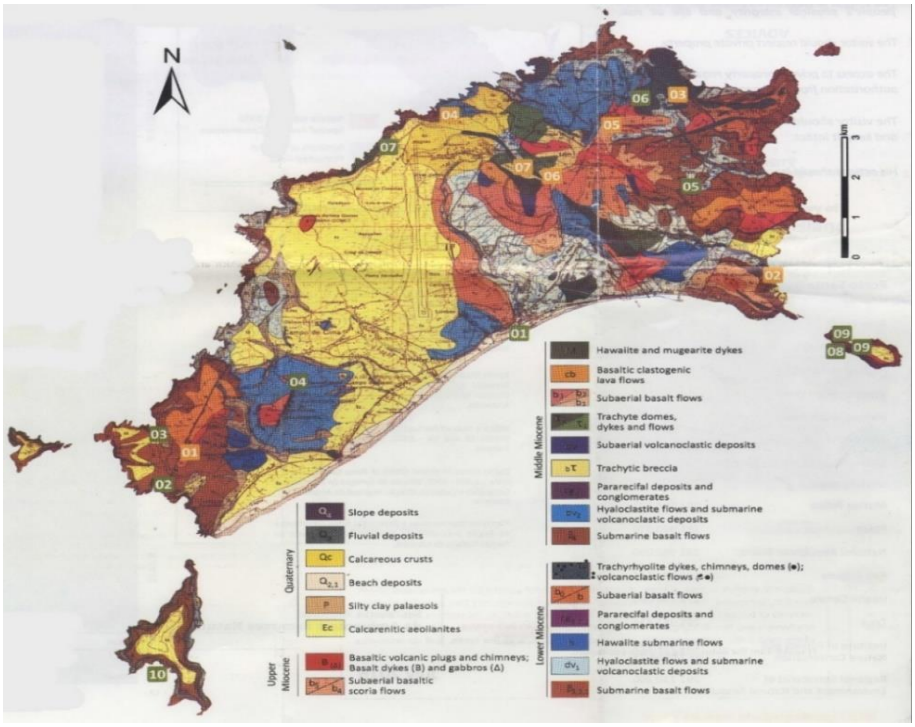

Figure 5 Geological map of Porto Santo [from (Ferreira & Neiva, 1996)]

2.1.1 Sedimentary Deposits

Sedimentary rocks cover about one third of the Porto Santo island, and include limestone rocks containing various fossils. Sedimentary deposits have been mostly formed by the marine platform developed around the island, from the Miocene to the end of the Würm glaciation (Ribeiro & Ramalho, 2010). Warm ocean water temperature and calcium rich basaltic rocks were the main factors leading to the growth of benthic organisms with a carbonate shell or skeleton (Ribeiro & Ramalho, 2010). The shells and skeletons of benthic organisms once accumulated at the base of the marine platform, driven by ocean water currents, were fragmented and deposited in specific locations, along with blocks of igneous rocks, forming breccias with limestone matrix. On the other hand, erosion led to disintegration of shell, and formation of bioclastic sands. Finally, the wind from the north direction, transported sediments to the sheltered regions of the onshore part of the island (Ribeiro & Ramalho, 2010).

Several types of sedimentary rocks with a wide range of importance are present on the island. The geological map (Figure 5) from Ferreira & Neiva (1996) illustrates the distribution of deposits contemporaneous with the submerged phase of the island. The fossiliferous limestone breccias and the sandy limestones and marls, as well as deposits from the Quaternary: carbonate eolianite, sands from unconsolidated dunes, limestone crusts and beach, slope and alluvial deposits are major sedimentary rocks present on the island. Calcarenite eolianites and sand from unconsolidated dunes are best suited to have aquifer properties. Limestone, if weathered can allow preferential pathways for water flow. Beach sands may be permeable depending on the compaction level of grains.

2.1.1.1 Fossiliferous Limestone Breccias

Fossiliferous limestone breccias with high coral content occur throughout the island in outcrops distributed along the same altitudes attached to volcanic rocks. These are formed by the accumulation of detritic elements from those same rocks and bioclastic elements, with carbonate cement. These rocks contain large amounts of fossils, mostly corals that can reach of significant size (Ribeiro & Ramalho, 2010). The fossils geochronology suggested that fossiliferous limestone breccia dates to Miocene. The reported fossils correspond to warm and shallow waters marine organisms, and the sediments resulted mainly from the accumulation of their skeleton fragments (Ribeiro & Ramalho, 2010).

2.1.1.2 Sandy Limestones and Marls

The sandy lime stones and marls are very locally present on the island. They outcrop at Ribeira da Serra de Dentro, close to the village of Serra de Dentro. The site has thick layer of sandy limestones (Figure 6) and yellowish marls, with fossils (Figure 7) and spherical concretions of calcified algae [locally known as “laranjas” (Figure 8), meaning oranges], followed by levels of conglomerates, mudstones and conglomeratic limestones.

Figure 6 Lime stone deposits of Porto Santo

Figure 7 Sandy Limestone with Calcified algae

2.1.1.3 Dunes

The consolidated and unconsolidated units of calcareous dunes are the biggest sedimentary formation of the island. The consolidation of dunes has occurred by dissolution of calcium carbonate from the marine calcite rich shells and its deposition in the spaces between grains, and cementing them. The consolidated dunes are present at several sites in the central zone, although the best places where its internal structures can be seen are the coastline outcrops, particularly in the north and south sectors of Porto dos Frades and near Fonte de Areia (Figure 9). The unconsolidated carbonate dunes of fine to

medium size grains, consists mostly of shell fragments and minerals weathered minerals from volcanic rocks.

Figure 8 Calcified Limestone, locally named as "Laranjas" on the island

Figure 9 Eolianites of Fonte De Areia, wind eroded faces are distinctly visible

2.1.1.4 Limestone Crusts and Beach, Slope and Alluvial Fan Deposits

Limestone crusts consist of thick calcrete sequence (Figure 6), formed by pedogenic processes similar to those consolidated dunes. They are found throughout the island, and are particularly visible in many road outcrops. They are mostly found west and north of Camacha.

The island has a 7 km long sandy beach of fine grained white sand and is one of the most attractive location of Porto Santo. The beach deposits (Figure 10) have been formed by remobilizing the dunes material by wind and rain water, and depositing them close to the coast.

Figure 10 Beach deposits of Porto Santo

The slope deposits, present mainly close to the beach deposits, are composed of coarse-size materials, resulting from the weathering of pyroclastic rocks, but contain blocks of all types of volcanic and sedimentary rocks on the island, even dune rocks and fossiliferous breccias.

Alluvial fan deposits are scarce and occur in the beds of the streams, especially in the Southeastern part of the island.

2.1.2 Igneous Rocks

Igneous rocks present on the island corresponds to two volcanic history: the submarine and subaerial phases of volcanism. The submarine sequence consisting of basaltic and trachybasaltic flows interlayered with pyroclastites and hyaloclastites, and other volcaniclastic deposits dates to more than 14.2 million years and the subaerial sequence of volcanism dates between 14.2 and 8.3 million years (Figure 11).

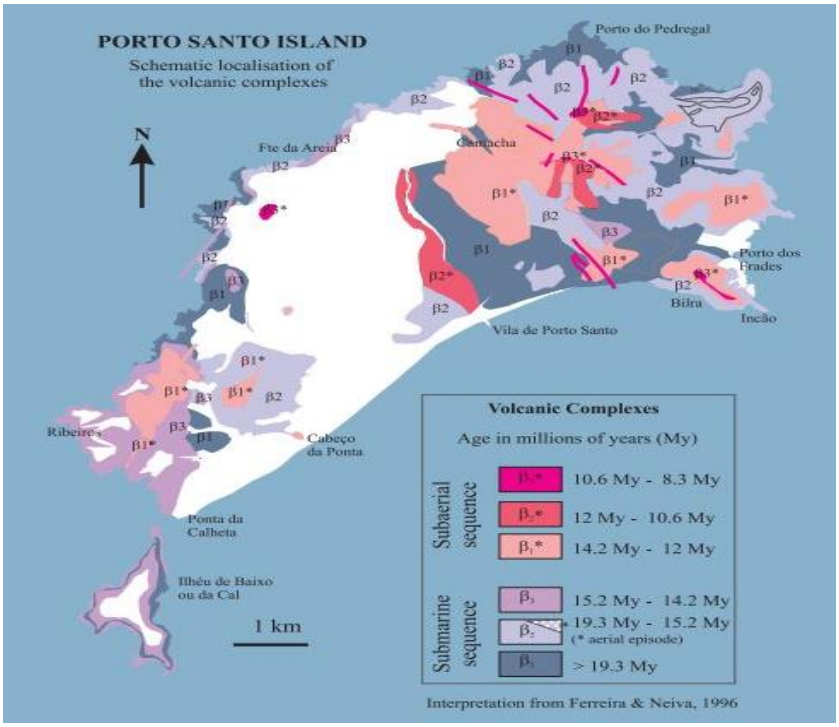

Figure 11 Schematic localization of volcanic complexes [from (Ribeiro & Ramalho, 2010)]

2.1.2.1 Submarine Sequence

Trachytic submarine volcanism on the island is represented in the form of non-vesicular pillow lobes of trachyte, which points to anomalously hot nature of trachyte magma (Figure 12). Pillow lobes of varying dimension have penetrated the underlying basaltic hyaloclastites. Generally, pillows are more extensive in longitudinal section. Trachyte pillow lobes are extensive present in northeastern and southeastern Porto Santo (Schmidt & Schmincke, 2002).

Figure 12 Pillow lavas observed in the submarine sequences of Zimbralinho

Southwestern tip of Porto Santo preserves the spectacular example of submarine basaltic activity, where almost vertically orientated to slightly inclined layers of basalt set in a hyaloclastite breccia. Many dikes terminate into pillow shaped (Figure 13). Dikes protuberance results to numerous thin and imbricated slabs with single sheets of a few meters in lateral extent. Slabs are dissected by small normal joints and form convex upward curves (Schmidt & Schmincke, 2002).

Figure 13 Basaltic dike connected to a small submarine compound pillow in southwestern tip of Porto Santo

2.1.2.2 Subaerial Sequence

The subaerial volcanic eruptions typically produce sub-horizontal lava flows and associated with mass wasting process at all growth stages of Porto Santo (Schmidt & Schmincke, 2002). Scoria cones of Porto Santo are inferred to have been formed by pyroclastic fragmentation of basaltic magma, because of explosive activity in the subaerial setting and later shaped in the present form by transport action of the wind (Schmidt & Schmincke, 2002).

Subaerial tuff rings (Figure 14) formed during phreatomagmatic volcanic eruptions are abundant along the coast of volcanic island (Vespermann & Schmincke, 1999). Schmidt & Schmincke (2002) have reported the erosional remnant of a tuff ring with an estimated thickness 40-50 meters in an inaccessible vertical cliff section at the eastern coast of Porto Santo. Binocular observations concluded that the tuff ring remnants are yellowish, fine-grained, thinly bedded, and underlie scoria cone deposits.

Figure 14 Scoria cone present in northwestern side of Porto Santo

Pico de Ana Ferreira, present on the southern part of the island, hosts outcrop of trachytic hexagonal columnar joint (Figure 15). The joints, exposed by the activity of an old quarry, resulted from the development of shrinkage surfaces during cooling and crystallization of the magmas.

Figure 15 Trachytic dyke of Pico de Ana Ferreira

2.2 Geomorphology of Porto Santo

Due to its geochronological antiquity and deep dissections, caused by prolonged exposure to vertical and horizontal erosion mechanisms, the island represents a marked erosion of relief forms. Porto Santo island is located 40 km northeast of Madeira, where erosion is considered as the main agent responsible

for the dismantling of the volcanic structures, and being particularly associated with the geological constitution and the evolutionary context.

From geomorphological perspective, the island is comprised of two volcanic mountain systems located at the northeast and southwest ends (Figure 16), and separated by an extensive depressed, flattened and tilted platform for the southeast, of sedimentary nature. The rugged rocky edges and cliffs includes Pico do Castelo (437 meters), Pico do Juliana (447 meters), Pico do Gandaia (499 meters) and Pico do Facho (517 meters).

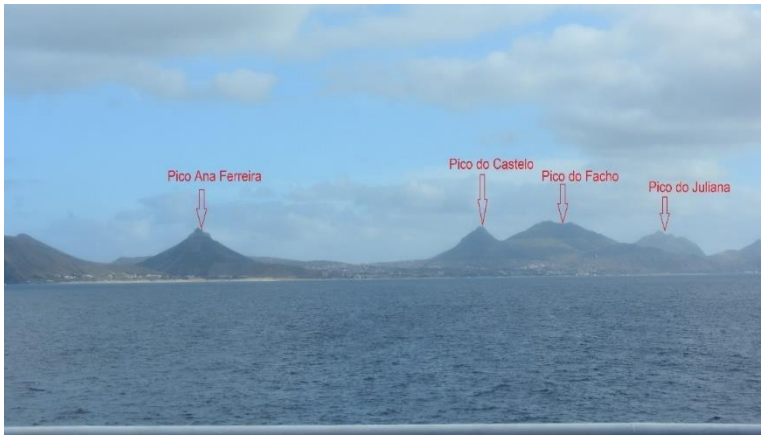

Figure 16 Major peaks of Porto Santo

The coastal plain in the central portion includes a long white sandy beach (Figure 17) and the low-lying areas. This area is covered by fine grained sediments, mainly deposited by winds. About 40% of the island area is below 50 meters of elevation while major landmass (54%) is having elevation between 50-200 meters (Figure 18).

Figure 17 Coastline of Porto Santo

Undulating topography of the island deeply affects the stream channels, and presents very different hydrological and hydrographic characteristics. Thus, considering the dearth of flora encrust and the present precipitation regime, characterized by intense rainfall, in a short period of time, the drainage network exhibits a torrential flow regime, of a temporary character. The water flow in channels are characterized by a high load capacity and a strong energetic gradient, thus contributing to the carving of vigorous runoff grooves.

The stream systems of Ribeiro do Calhau and Serra de Dentro are present in the eastern side of Porto Santo, with a marked longitudinal slope of 14.2% and 17%, respectively. Considering the problem of existing high slope and the resulting nature of flow, structural measures of torrential flow reduction in the form of in channel dikes were adopted by Madeira Regional Water Plan, in order to promote the reduction of the potential erosion and transport capacity of the external agents and, consequently, to contribute to retention of material and to the minimization of ravine processes (Naturais, 2016).

With a uniform distribution, the stream network of the Porto Santo island presents a northwest-southeast orientation, falling in line with the general slope of the topographic surface. Streams are more likely straight water lines, with the exception of Ribeiro do Tanque, which presents a sinuosity index of 51.5%, and with an orientation approximately perpendicular to the coastline.

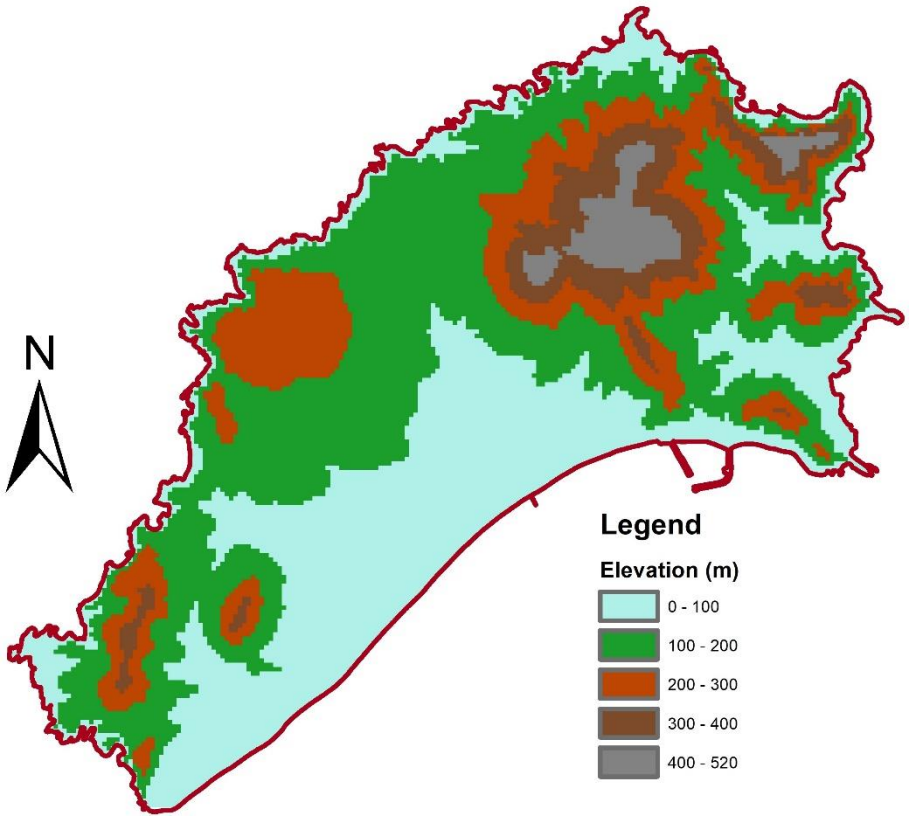

Figure 18 Hypsometric map of Porto Santo

Table 1 Summary of physical characteristics

Parameters	Measurements
Average altitude	111 m
Highest peak	Pico do Facho (517 meters)
Average slope	30.4%
Perimeter	41 km
Area	42.2 km
Predominant soils	Calcissoles (40%)
Highest Length	12 km
Highest Width	6 km
Population	5483 inhabitants

2.2.1 Vegetation

The primitive floral species of arboreal and shrub types that covered the whole island since its discovery in 1419 are currently present at very few places (Silva, 2002). Deforestation practice adopted by the people of island since initial times for wood and agricultural land has transformed the island into semi-arid region. The consequences of the deforestation were mainly seen in the ecosystem and the resulting desertification of the island. The erosion on slopes and valley were highly activated due to loss of vegetation and resulted in the decrease in the thickness of the arable soils. During 1950's, the reforestation program was started on the island. Plantation of exotic species, especially pine of Aleppo (*Pinus halepensis*), Monterey pine (*Pinus radiata*), meager pine (*Pinus pinaster*) and Monterey cedar (*Cupressus macrocarpa*) has been done (Silva, 2002).

Present forest cover is limited to some clumps, and cover some ravines and inaccessible cliff. According to Meneses (1914), Porto Santo possesses two zones or regions of vegetation. The first one is called "maritime", extending from the sea level up to the heights of 200-250 m, represented by plants spontaneously distributed of the genera *Asphoderus, Convolvulus, Crepis, Emex, Erodium, Euphorbia, Fumaria, Lotus, Scorpiurus, Lycium, Mesembryantemum, Salsola*, etc. The second zone of vegetation named "mountainous", covers (Figure 19) from the higher end of maritime zone up to the altitude of 517 m.

The noted species includes *Citysus, Lotus, Sedum, Myosotis, Mint, Origano, Sideritis, Saxifraga, Galium, Senecio, Sibthorpia, Parietaria, Dactylis, Festuca, Trifolium, Galactites, Sonchus, Echium, Erica, Plantago, Phyllis, Davallia*, etc.

The current land practice in the island for agricultural use is limited up to 200 meters of altitude only. The agricultural practice is not very intensive, and wheat, rye and barley are mainly grown there. Horticulture crops (Figure 20), commonly grown by seeds includes normal and sweet potatoes, beans, watermelons, lemons, etc. while vineyards (Figure 21) and fruits includes the year long. Vineyards adds to the economic activities of the local farmers where they prepare indigenous wines on the island itself.

Figure 19 Mountainous vegetation of Porto Santo

Figure 20 Horticultural farming on the island

Figure 21 Perennial vineyards plantation of Porto Santo

2.3 Hydrogeology

The intricate geological setting of Porto Santo, where less permeable volcanic rocks predominates in whole north and south western portion giving rise to steep slope promotes surface runoff, limits groundwater recharge and groundwater storage availability. Carbonate eolianite deposits and coastal sands present in the western and central part of the island possesses the infiltration potential but limited rainfall and high evapotranspiration rates objects the recharge process.

From hydrogeological point of view, the island has been classified into four different permeable units (Ferreira & Neiva, 1996). Carbonate eolianite, the largest permeable formation (Figure 22) situated in the western and central locations of the island, embodies varied nature volcanic rocks and at places carbonated sediments of mobile nature. Hydraulic conductivity of the aquifer may vary between 10^{-9} to 10^{-6} m/s, and has been categorized as less permeable depending on grain size and its compaction level. Carbonate, which is very perceptive to rainwater infiltration, manifest karstification event which allows infiltration. Few number of smaller streams originating from the higher elevation part of southern portion ends up in this carbonate eolianite formation before reaching to the sea indicating appreciable infiltration capacity of the formation at places. Presence of hard rocks basement below the carbonate eolianites does not allow deep percolation of water and results into springs at several places on the island. Arid climatic condition and proximity to salinity source aided by karstification make an easy pathway for sodium chloride laden Atlantic aerosols to circulate into the aquifers and adds to groundwater salinity hazard persisting over the island.

Second unit to be considered as an aquifer is beach sands formation having porosity values between 0.35 to 0.40, depending upon compaction level. Permeability measurement in the aquifer varies between 10^{-6} to 10^{-5} m/s, and has been categorized as low to medium depending on predominance of clay content and grain size variation (Silva, 2002). Noting the unit thickness, variable permeability and

presence of formation mostly in unsaturated zone rates it as of inferior quality. This formation serves as a pathway for recharge of underlying volcanic formation which is found mostly below carbonate eolianite cover (Silva, 2002). This beach sands formation also serves as an easy course for streams originating in the northeast portion of island to end up to the sea. This formation has highest threat for salinity ingress owing to its proximity to the sea and, also because of high groundwater abstraction by the nearby hotels for gardening and other purposes.

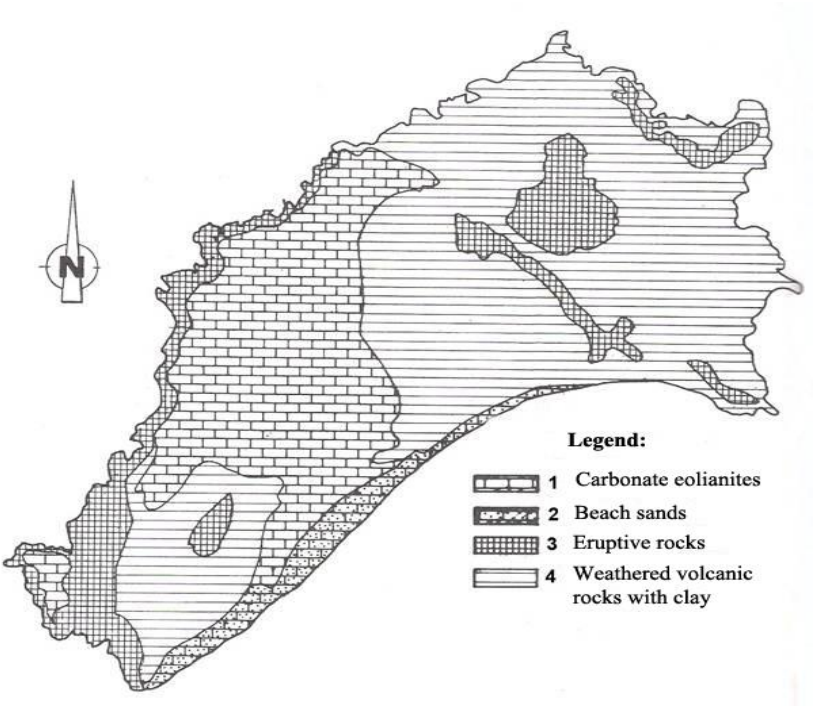

Figure 22 Major aquifers of Porto Santo island [from (Ferreira & Neiva, 1996)]

Weathered volcanic sequence whose crust consist mainly of colluvium and quaternary alluvium deposit host several perched aquifers. Presence of hard rocks beneath the quaternary deposit gives rise to number of springs which is tapped for the use on the island. Perched water body and the springs have resulted from the variable porosity and permeability along the subsurface zone which restricts the infiltration. Higher clay content in the weathered volcanic sequence have lessened the porosity and permeability, and results in less infiltration into subsurface. The reduction of porosity and permeability have its after effect in the form of increased surface runoff on the island. Lack of water holding capacity in this formation is also reflected by the absence of vegetation in the high land areas. Volcanic rocks in the form of basalts, rhyolite and trachyte are fractured at places but filling of fine particles do not allow much of infiltration (Silva, 2002) and thus not a productive zone for groundwater storage and abstraction.

2.4 Conceptual Groundwater Flow Model

Water table elevation measurement of any location gives us the idea about the groundwater head in the area. Minimum three points are required to know the general direction of groundwater flow. Water level measurement of wells, boreholes and springs of Porto Santo island have been plotted to know the

general direction of groundwater flow on the island. The data points are not located homogeneously along the whole island. Very few number of wells and boreholes are present on the island and majority of them are near the east and south-eastern coast. All wells were dug to shallow depth, ranging between 10 to 35 meters of depth only. Water level in the wells varied between one meters below surface level close to the eastern coast to 30 meters below surface in higher elevation areas. Presence of springs are not very uniform on the island or are inaccessible at some locations. North and central part of the island has very few number of data points to account the true behavior of groundwater movement. The spatial variation of data is more uniform in the northeastern, southeastern and the sandy beach areas.

In case of wells, depth of water level from the ground surface has been subtracted from the ground elevation to know the water head at that place while the surface elevation of the spring locations has been treated as local head. The general direction of water movement duplicates the topography at most places. At higher relief areas, the water table is at higher elevation from the sea level while it approaches up to one meters above mean sea level close to the coastline of Porto Santo (Figure 23). The northeast part of the island shows a clear gradient towards the lower relief portion. The groundwater flow is following the topography gradient and the water level head decreases from 120 meters above mean sea level to 40 meters above mean sea level.

Central portion of the island which covers the carbonate eolianite formation has three kinds of flow behavior. From the north portion of the island some flows are directed towards the central which may due to difference in topography. From the southern portion also, a part of flow direction is towards the central island. This flow direction is synchronous with the small streams originating in the southern highlands of the Porto Santo which ends in to the carbonate eolianite formation. A third kind of flow pattern from northwest to southeast is visible in the central portion indicating flow of groundwater from higher elevation to the beach sands formation.

All along the beach sands formation, the general direction of groundwater flow is towards the sea. The hydraulic head has decreased in beach sands formation as compared to the rest of the island. The groundwater head in beach sands formation is the range of 1-10 meters above mean sea level. Based on the water table head decline towards the southeastern and eastern coast, this could be a potential area of submarine groundwater discharge from the island of Porto Santo, but no volumetric data is available at this stage.

Lower hydraulic gradient along the beach sands formation which also hosts maximum number of wells is highly vulnerable in terms of salinity intrusion from the sea water ingress. Ferguson & Gleeson, (2012) have examined the relative vulnerability of coastal aquifers to sea level rise and emphasised that the impact of groundwater abstraction on coastal aquifers is more significant than the impact of sea-level rise or changes in groundwater recharge. In case of Porto Santo, where groundwater abstraction wells are located with in 1 km distance from coastline, the vulnerability is supposed to be more exacerbated during the summer season when the water demand increases due to sudden increase in the number of tourist.

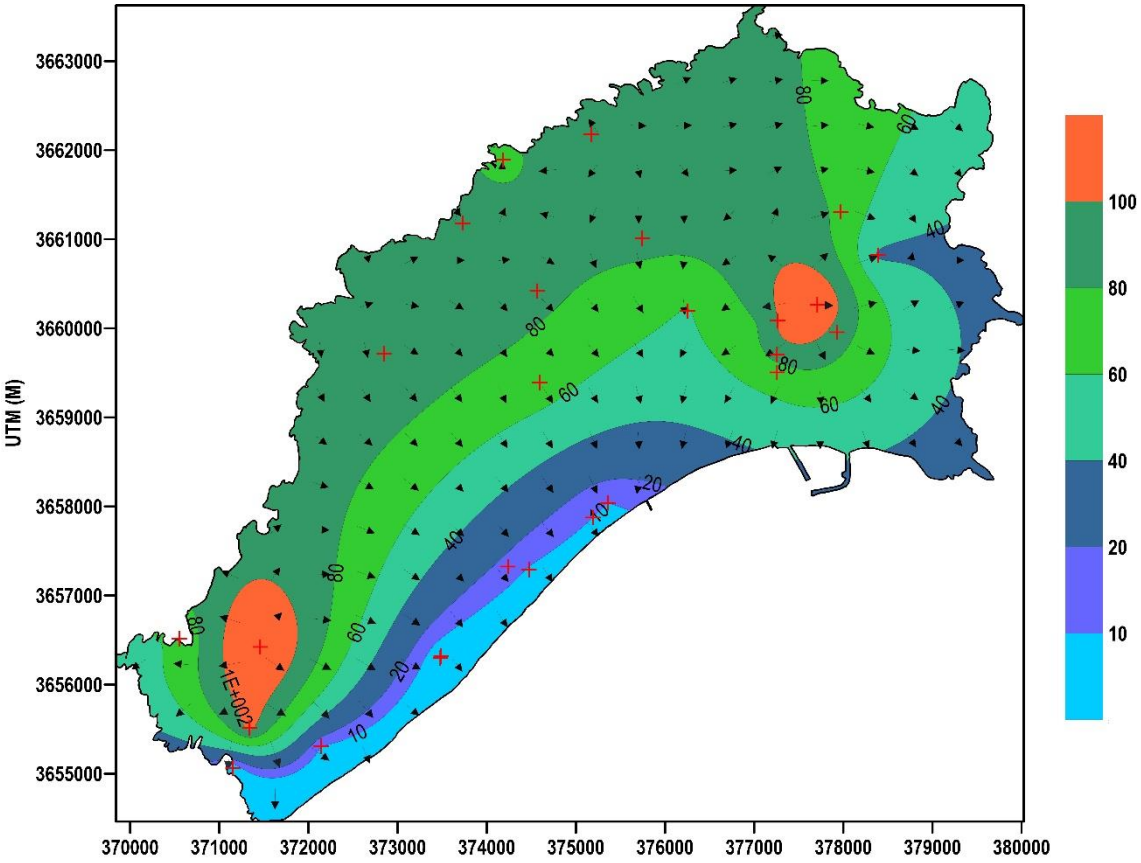

Figure 23 Water table elevation (meters above sea level) map of Porto Santo

CHAPTER

3

Groundwater Recharge

Groundwater recharge is the amount of water coming either from rain or surface which reaches the permanent water table either by direct contact in the riparian zone or by downward percolation through the vadose zone. Groundwater recharge is the quantitative volume of water which, in the long term, is available for both abstraction and supporting the baseflow component of rivers (Rushton & Ward, 1979). The measurement of net effective rainfall, the amount of rainfall remaining after evapotranspiration, and the fractionation of this hydrological excess water between surface water and groundwater is an important consideration for water balance. Methods for estimating direct and indirect recharge to the groundwater table, through pores in unconsolidated terrain and via fractures and fissures in hard rock or limestone terrain, as localized infiltration below water-filled surface depressions or as lateral runoff to an aquifer at the edge of a confining layer, are discussed in detail by Lerner *et al.,* (1990), Kitching *et al.,* (1980) and Kitching & Shearer, (1982).

3.1 Climate

Porto Santo has temperate oceanic semi-arid climatic, which is influenced by its location, relief, dimension and altitude. Due to its presence in the subtropical high-pressure region of the Atlantic, the island is subjected to yearlong northeasterly winds. The weather conditions are more influenced by the Azores anticyclones rather than the Atlantic polar fronts and the anticyclonic scenario developed in the northwestern portion of the Africa and the western European continent. The diurnal variation in temperature, relative humidity, wind, cloudiness and precipitation are related to the small size of the island and its proximity to the Madeira island that constitute its surrounding orography. For quantitative weather parameters measurements, a weather station has been established at the Porto Santo airport (Latitude: 33º 04' N, Longitude: 16º 21' W and Altitude: 78 m) by the Institute of Meteorology, Regional Delegation of Madeira (IPMA), and is considered the representative of the whole island. The data for main climatic parameters like temperature, relative humidity, atmospheric pressure, precipitation, evaporation, potential evapotranspiration, insolation and wind data are available for 2008-2016.

3.1.1 Air Temperature

The monthly averaged value of air temperature for the study region is shown in Figure 24. Summer months have recorded the average maximum temperature mostly above 20°C and goes even beyond 25°C in August and September. Highest average maximum temperature on the island has been recorded in the August month. Very little variation is recorded in average maximum temperature during

winter months. observational period. Both summer and winter season have witnessed increase as well as decrease for the absolute maximum temperature.

February month has recorded the average minimum temperature of all the observation period (Figure 24). Excluding three initial months of the year, the average minimum recorded temperature is above or close to 15°C. The monthly average temperature for all months fluctuates between 15-25°C. The temperature, without any extremities, attracts large number of tourist on the island.

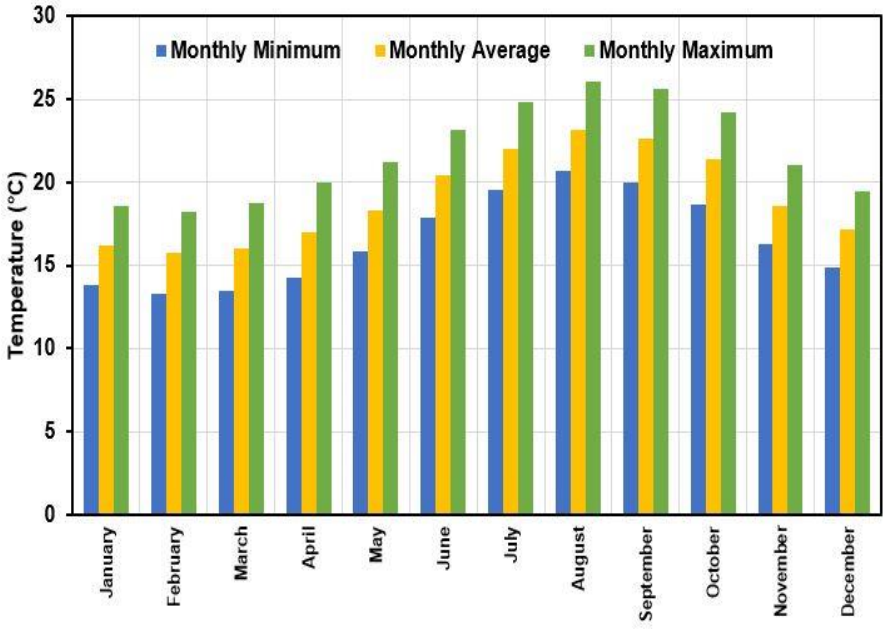

Figure 24 Monthly averaged value of air temperature in the study region (Source: IPMA)

3.1.2 Precipitation

The mean annual precipitation value for the period 2008-2016 is 457 mm per annum (Figure 25). The present value is 70 mm higher than reported by Silva (2002) for the period 1961-1990. This precipitation amount characterizes Porto Santo as a region of low precipitation, typical of anticyclones, where the processes of evaporation and transport predominate. The statistics indicate that November and December are the wettest month while it rains very little during summer months. Between May to September, only 15% of the total precipitation occurs, and rest falls during October to April in form of extreme events most of the time.

3.1.3 Evaporation

The average monthly evaporation value has been calculated based on the daily evaporation data available through IPMA source from open pan method. The average monthly evaporation value for all measured months are higher than the average monthly precipitation (Figure 26). For the period 2008-2016, the average annual evaporation is 3.2 times higher than the precipitation amount. Highest recorded evaporation value is from August month which receives least precipitation while lower evaporation values have been recorded during winter months.

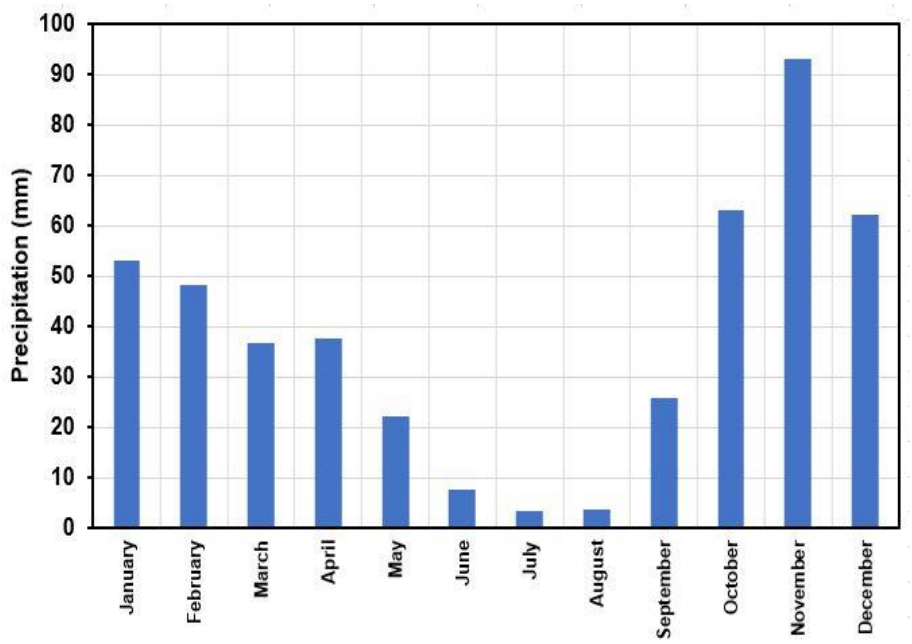

Figure 25 Average monthly precipitation value of Porto Santo (Source: IPMA)

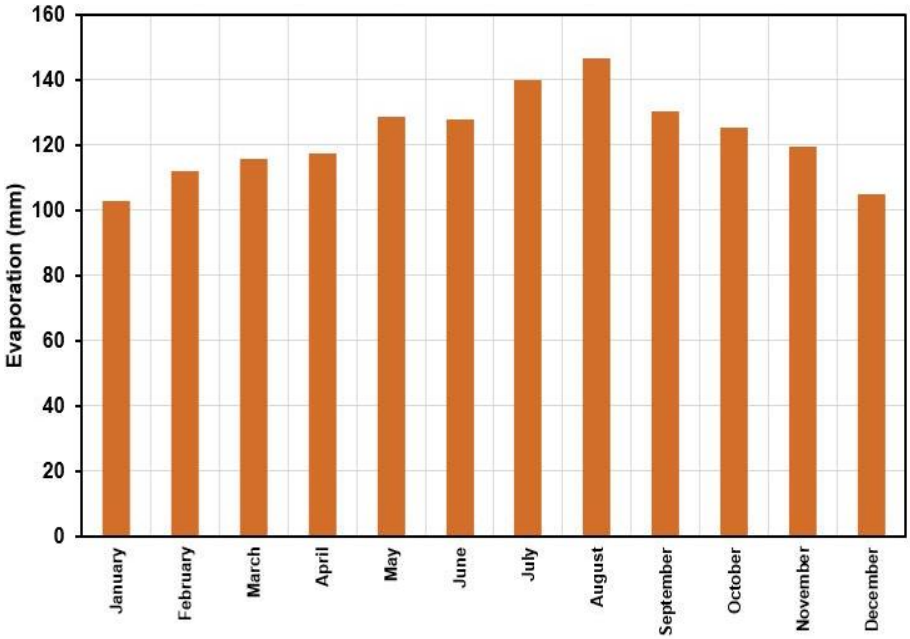

Figure 26 Average monthly evaporation value using Pan evaporation method (Source: IPMA)

3.1.4 Potential Evapotranspiration

Potential evapotranspiration refers to the amount of evaporation that would occur if a sufficient water source is available. The actual evapotranspiration is the result of atmospheric demand of moisture from a surface and the ability of the surface to supply moisture, while potential evapotranspiration is a measure of demand side from the environment. Saturated soils yield to the atmosphere either by direct evaporation from the soil layers or transpiration through plants.

To calculate potential evapotranspiration, both direct and indirect approach has been used. Direct approach includes evaporation from open pan while indirect includes the Penman (1948) and Thornthwaite (1948) equation. Pan evaporation gives average of 1471 mm per annum which is 3 times higher than the average precipitation for same time period. Other thwo indirect methods gives highly variable results. Thornwaite calculation yields to 889 mm per annum while Penman method yields 1887 mm per annum, which is highest of all three (Figure 27).

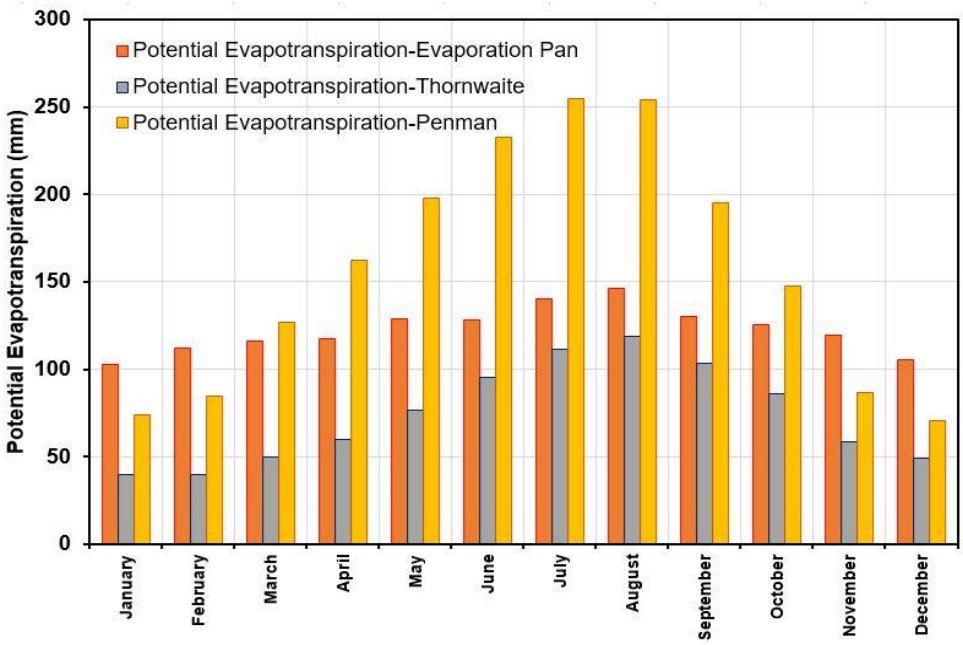

Figure 27 Average monthly potential evapotranspiration values between 2008-2016

3.1.5 Relative Humidity of Air

Relative humidity is the measure of the amount of moisture in the air as compared to what the air can hold at that particular temperature. It is expressed in the percentage form. The island's relative humidity for year 2008-2016 shown in Figure 28 has very little variation over the annual cycle. Throughout the year, the average monthly relative humidity is more than 72 %, while the highest observed value is approximately 78 % indicating that the air is neither too dry nor too much moisture laden.

3.1.6 Insolation

Solar insolation is basically the measure of solar radiation on the surface of the earth. Average hours of monthly insolation for year 2008-2016 varies throughout the year. The maximum monthly average hours value of insolation was recorded in August, and it plateaus around the summer months (Figure 29). The summer months have recorded an average 60% of sun during the whole day length. The average monthly insolation during winter season for 2008-2016 was 135 hours per month and accounts to 43% of the total day length time.

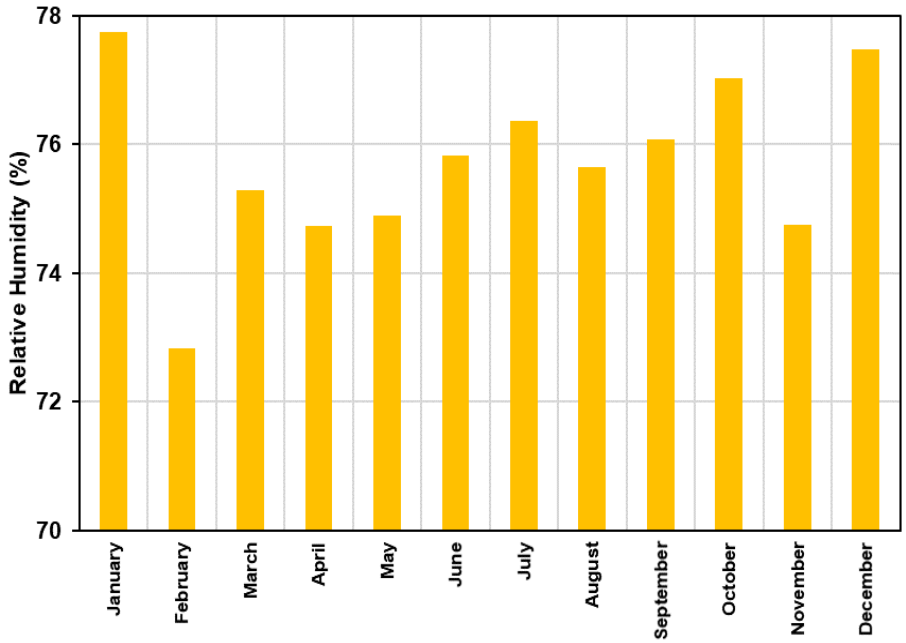

Figure 28 Average monthly Relative Humidity value for the study region (Source: IPMA)

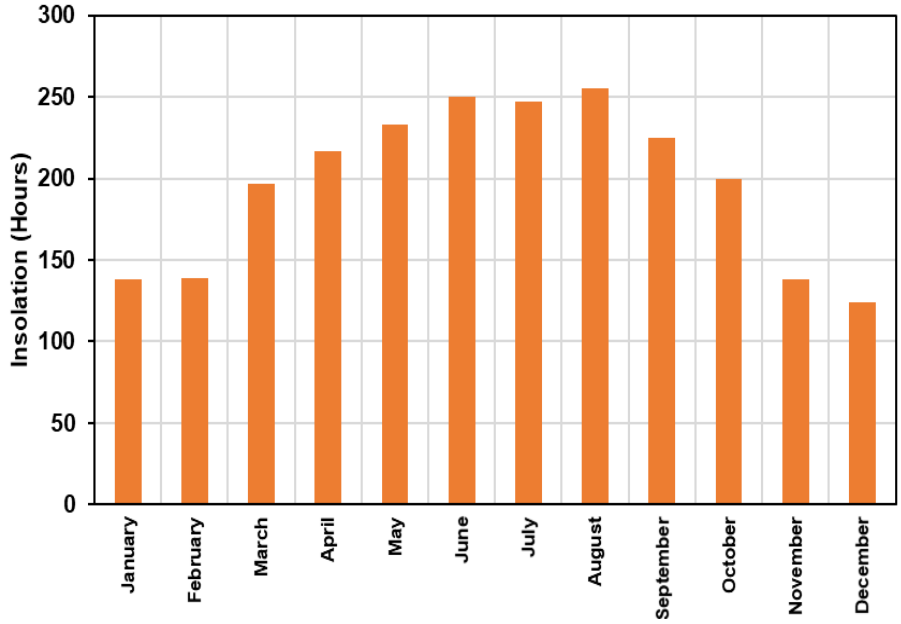

Figure 29 Monthly average solar insolation value for the study region (Source: IPMA)

3.2 Groundwater Recharge Estimation

Two methods of groundwater recharge estimation have been used to approximate groundwater recharge in Porto Santo aquifer. Penman-Grindley is a physical method while Chloride Mass Balance is a geochemical method applied both to the saturated and unsaturated zones. A summary of the methods used is presented in the following sections.

3.2.1 Penman-Grindley method

The trivial approach of calculating recharge using a soil water budgeting method is based on the studies of Penman and Grindley (Penman 1948, 1949; Grindley 1967, 1969). The method works on simple concept that water is held in as soil moisture, precipitation adds to the storage and evapotranspiration depletes it. When soil moisture storage is full, the excess water routes to either subsurface to become part of groundwater storage or to the surface to continue as runoff.

The storage change is based on simple water balance model:

$$P = ET_R + R + \Delta S \quad [1]$$

$$\Delta S = P - ET_R - R \quad [2]$$

where P is rainfall [L], ET_R is the real evapotranspiration [L], R is the runoff [L^{-1}] and ΔS is the change in soil water storage [L].

The most tedious task is to calculate real evapotranspiration (ET_R). Pan evaporation method or irrigated lysimeters are two direct procedures of ET_R calculation, while Penman (1948) and Thornthwaite (1948) can also calculate the ET_R based on soil moisture budgeting approach.

The Penman-Grindley method has been used to estimate the groundwater recharge in Porto Santo island. Water budgeting is based on rainfall data from Porto Santo airport meteorological station. Other climatological parameters (temperature, wind velocity, insulation, humidity) has been collected from same site to calculate the potential evapotranspiration. Potential evapotranspiration measurement through Pan evaporation method, Penman and Thornthwaite formulae from the preceding chapter has been used here for groundwater recharge calculation.

Assuming that the maximum volume of water stored for plants use is equal to 100 mm and that the volume of water stored at the beginning of the hydrological year in October is zero, a sequential water budget has been carried out for the three values of potential evapotranspiration. The results obtained are summarized in Table 2 Water Budget for Porto Santo using Penman, Thornwaite and Pan evaporation potential evapotranspiration.

The water budget calculation using all three methods shows that from the 457 mm of rainfall, all of it is lost through evapotranspiration. The calculated potential evapotranspiration through either method is between 1.9-4.1 times of precipitation on the island. All methods have yielded water deficit in the soil zone and concludes to null groundwater recharge on the island. The results obtained through three above mentioned process is contradictory to the local condition of the island. Several low yielding springs are present in all major geological formation of the island. In the absence of recharge, they may have dried up. Also, the recharge is happening in the most productive carbonate eolianite formation through karstification process which is confirmed by the vanishing of small streams originating from the southern highlands in the carbonate eolianite formation. Above mentioned facts point the limitation of soil water budgeting in semiarid conditions.

Table 2 Water Budget for Porto Santo using Penman, Thornwaite and Pan evaporation potential evapotranspiration

	OCT	NOV	DEC	JAN	FEB	MAR	APR	MAY	JUN	JUL	AUG	SEP	Total
Using Penman potential evapotranspiration													
P	63.0	93.0	62.1	53.0	48.3	36.7	37.7	22.1	7.7	3.4	3.8	25.9	456.8
PET	147.4	86.6	70.7	74.2	84.8	127.0	162.3	198.1	232.3	254.5	254.2	195.2	1887.2
P-PET	-84.4	6.4	-8.5	-21.2	-36.5	-90.3	-124.5	-176.0	-224.6	-251.1	-250.3	-169.3	-1430.4
RET	63.0	86.6	68.5	53.0	48.3	36.7	37.7	22.1	7.7	3.4	3.8	25.9	456.8
Rx	0.0	6.4	0.0	0.0	0.0	0.0	0.0	0.0	0.0	0.0	0.0	0.0	6.4
EXC	0.0	0.0	0.0	0.0	0.0	0.0	0.0	0.0	0.0	0.0	0.0	0.0	0.0
DEF	84.4	0.0	2.1	21.2	36.5	90.3	124.5	176.0	224.6	251.1	250.3	169.3	1430.4
Using Thornwaite potential evapotranspiration													
P	63.0	93.0	62.1	53.0	48.3	36.7	37.7	22.1	7.7	3.4	3.8	25.9	456.8
PET	86.2	58.8	49.1	39.9	40.0	49.9	59.9	76.5	95.2	111.4	118.7	103.1	888.8
P-PET	-23.1	34.2	13.0	13.1	8.3	-13.3	-22.2	-54.4	-87.5	-108.1	-114.9	-77.2	-432.0
RET	63.0	58.8	49.1	39.9	40.0	49.9	37.7	22.1	7.7	3.4	3.8	25.9	401.4
Rx	0.0	34.2	47.2	60.3	68.6	55.3	33.1	0.0	0.0	0.0	0.0	0.0	298.7
EXC	0.0	0.0	0.0	0.0	0.0	0.0	0.0	0.0	0.0	0.0	0.0	0.0	0.0
DEF	23.1	0.0	0.0	0.0	0.0	0.0	22.2	54.4	87.5	108.1	114.9	77.2	487.3
Using Pan evaporation potential evapotranspiration													
P	63.0	93.0	62.1	53.0	48.3	36.7	37.7	22.1	7.7	3.4	3.8	25.9	456.8
PET	125.3	119.4	105.1	102.9	112.0	115.9	117.5	128.6	127.8	139.9	146.6	130.2	1471.2
P-PET	-62.2	-26.4	-43.0	-49.9	-63.8	-79.2	-79.7	-106.5	-120.1	-136.5	-142.7	-104.3	-1014.4
RET	63.0	93.0	62.1	53.0	48.3	36.7	37.7	22.1	7.7	3.4	3.8	25.9	45.8
Rx	0.0	0.0	0.0	0.0	0.0	0.0	0.0	0.0	0.0	0.0	0.0	0.0	0.0
EXC	0.0	0.0	0.0	0.0	0.0	0.0	0.0	0.0	0.0	0.0	0.0	0.0	0.0
DEF	62.2	26.4	43.0	49.9	63.8	79.2	79.7	106.5	120.1	136.5	142.7	104.3	1014.4
Legend: P=Rainfall, PET=Potential Evapotranspiration, RET=Real Evapotranspiration, Rx=Water reserve for plant EXC=Runoff+stored, DEF=Water deficit													

3.2.2 Chloride mass balance in the unsaturated zone

Due to cost effectiveness and absence of any intricate methodology involved, the groundwater chloride mass balance (CMB) method is customarily used for calculating groundwater recharge. CMB methods does not require sophisticated instrumentation and calculates groundwater recharge independent of recharge methodology. The recharge estimates that are integrated in the spatial and temporal scale, and was originally applied in the late sixties to estimate recharge rates in the coastal plain of Israel (Eriksson & Khunakasem, 1969).

In order to apply CMB approach for recharge estimation three environmental variables should be known a priori, which are: (1) the long term mean annual rainfall for the study region; (2) the average annual

total chloride fallout for long term period; and (3) the average groundwater chloride concentrations in the study area.

The CMB method assumes that chloride is a conservative, non-adsorbed environmental tracer under steady-state conditions, and the validity of its application is restricted by several assumptions:

- The only source of chloride in groundwater is either from rainfall or from dry deposition, and recycling of chloride within the aquifer is not considered;
- Chloride fallout through rainfall and atmospheric deposition (wet and dry fallout) is considered to be constant over long periods of time;
- Rainfall is evaporated and/ or recharged to groundwater without any significant surface runoff;
- No groundwater evaporation occurs upgradient from the groundwater sampling points.

Allison & Hughes (1978) stated the basic equation to calculate the groundwater recharge through CMB.

$$\overline{q_R} = \frac{\overline{P}(\overline{C_P}+\overline{C_D})}{\overline{C_{gw}}} \quad [3]$$

where q_R is the annual recharge rate [L T^{-1}], P is the long-term mean annual precipitation [L T^{-1}], C_P is the weighted mean concentration of chloride in rainfall [M L^{-3}], C_D is the amount of chloride in the dry deposition [M L^{-2} T^{-1}] and C_{gw} [M L^{-3}] is the average chloride concentration in groundwater within the recharge area.

The average annual precipitation value of the island for 2008-2016 is 457 mm per annum. Average chloride concentration of 924 mg/L has been reported from the hydrochemical analysis from three field campaigns on the island. Due to absence of rainfall chloride concentration data from the Porto Santo island, the rainfall chloride data published by Naranjo *et al.,* (2015) of the nearby Gran Canaria island having similar climatic and physiographic setting as of Porto Santo has been used. While using the data from the nearby Gran Canaria island, the elevation of sampling point and precipitation amount has been taken into consideration, since elevation and precipitation amount can have a major influence on the chloride concentration in the collected rainfall. Average of rainfall chloride concentration from sampling location having altitude and rainfall amount synchronous with Porto Santo has been selected for the present study. The data adopted from Naranjo *et al.,* (2015) is given in Table 3 below:

Table 3 Results of atmospheric chloride bulk deposition in the area. Z = elevation; P = precipitation; C_P = precipitation-weighted average chloride concentration in rainfall during the study period

Zone	Station	Z (m. a. s. l.)	P (mm/year)	C_p (mg/L)
N2	036	375	264	21.9
N2	199	443	361	28.9
N2	055	577	581	12.9
N2	203	645	467	16.9
N3	088	315	296	20.6
N4	213	485	310	28.9

Assuming that the long term mean annual rainfall for the study region is 457 mm per annum and the average annual chloride deposition (including wet and dry deposition) in the area is 21.7 mg/L, the long-term groundwater recharge was calculated using Allison & Hughes (1978) equation. The infiltration rate of 11.4 mm per year is obtained for the island, corresponding to approximately 2.3% of the annual precipitation under present climatic situation.

3.4 Conclusions

Average annual temperature of Porto Santo is 19°C without any strong seasonality variation which makes it one of the pleasant tourist destination. Temperate climate is witnessed throughout the year. Based on the small precipitation amount, the island comes under semiarid region. In terms of precipitation, strong seasonality is witnessed. Summer months receives very low precipitation while winter months receives the major amount and mostly as high rainfall events. Irrespective of the season, the evaporation rate is very high on the island. Average annual potential evapotranspiration calculation using Penman, Thornwaithe and Pan evaporation yields higher value than the average annual rainfall received by the island.

Groundwater recharge calculation using soil water budget and geochemical method has given varying results. Soil water budget method is data intensive and the accuracy depends mainly on the evapotranspiration measurement. Over and/ or underestimation of evapotranspiration will direct impact the water budget. All three evapotranspiration values conclude to water deficit on the island. On the other hand, geochemical CMB method calculates 11.4 mm per annum as the groundwater recharge amount.

CHAPTER

4

Hydrogeochemistry

The study of groundwater quality requires the investigation of the main hydrogeochemical processes as they help to understand the controlling processes responsible for changes in groundwater chemistry, including water/ rock interactions, mixing processes and anthropogenic impacts. The geochemical properties of groundwater depend on the chemical composition of infiltrating water in the recharge areas as well as the different geochemical processes that are occurring in the subsurface along the main groundwater flow paths. These geochemical properties and processes may change seasonally and spatially and their study may be accomplished by investigating the chemical and isotopic composition of groundwater, through determination of ionic, molar and isotopic ratios, determination of residence times and calculation of saturation indices relative to most common minerals.

Groundwater quality in Porto Santo has been the subject of detailed hydrogeochemical studies during the present investigation. Geochemical data were collected to study the relations between the groundwater chemistry, aquifer mineralogy and patterns of groundwater flow. The results were used to optimize the use of groundwater for irrigation.

4.1 Sampling and Analytical Methods

4.1.1 Groundwater Samples

Groundwater samples were collected from all major identified geological formation during different field campaigns (Figure 30). Totally three filed campaigns were carried out in February and May 2008, and in April 2017. First two campaigns of year 2008 were carried out by Joao Baptista Pereira Silva and Maria Teresa Candesso de Melo and the results were published in Condesso de Melo *et al.,* (2008). Some groundwater chemistry data of February 2008 are from the project “Estudo hidrogeológico da caracterização e classificação da água subterrânea do Conjunto Turístico Colombo`s Resort, ilha do Porto Santo” by Silva *et al.,* (2008). A total of 52 samples including 36 from Condesso de Melo *et al.,* (2008) and Silva *et al.,* (2008) have been used for the present study. The sampling sites include fountains, shallow unconfined aquifer wells and boreholes spatially distributing over the whole island. For the groundwater sampling, a multiport flow-through cell connected in-line to the sampling points was used. Water samples were taken from the discharge point during pumping, once stabilization of the principal field parameters: pH, temperature (T), specific electrical conductance (SEC) and dissolved oxygen (DO) were observed.

The inorganic determinations, which includes the analysis of major, minor and trace elements of the samples for all field campaigns were performed at the Activation laboratories in Ontario (Canada). Isotopic analysis of samples from 2008 campaign only has been done. Stable isotope ($\delta^{2}H$ and $\delta^{18}O$) analysis of 24 and tritium (^{3}H) value determination of four samples were carried out at the Faculty of Science and Engineering laboratory in Rijksuniversiteit, Groningen (The Netherlands).

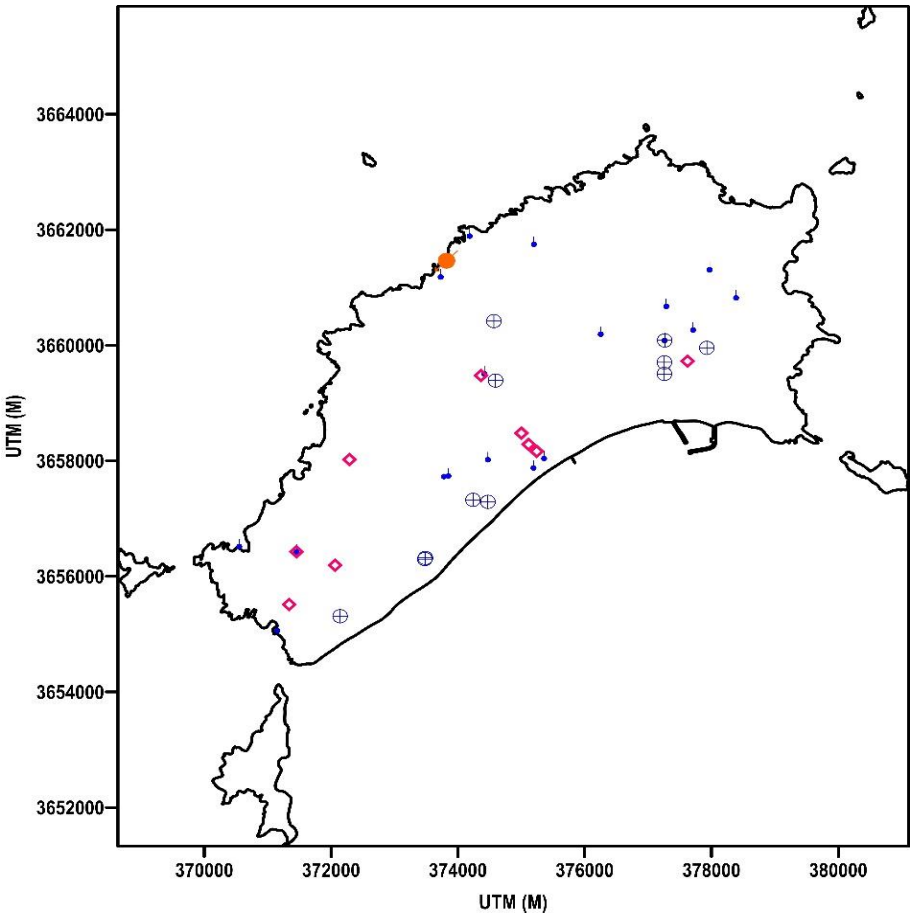

Figure 30 Groundwater and paleosol sample locations of Porto Santo (solid blue circle, rectangle, crossed circle and solid orange circle represents springs, mines, wells and unsaturated zone sampling sites respectively)

Deuterium and oxygen-18 results were reported as parts per thousand (‰) with respect to Vienna Standard Mean Ocean Water (VSMOW) using the standard δ (delta) notation (Gonfiantini, 1978). The analytical precision for stable isotope analysis is ±0.01‰ for $\delta^{18}O$, ±0.1‰ for $\delta^{2}H$. The concentrations of tritium are generally so small that tritium is reported in a special concentration called a 'tritium unit' or TU, defined as equal to 1 tritium atom per 10^{18} hydrogen atoms. The analytical precision for tritium is ±0.2 TU.

Electroneutrality was used as a quality control for all the determinations, and ionic mass balances with errors between –10% and +10% were considered to be acceptable. Ionic charge imbalances in most samples were less than 10% (Figure 31).

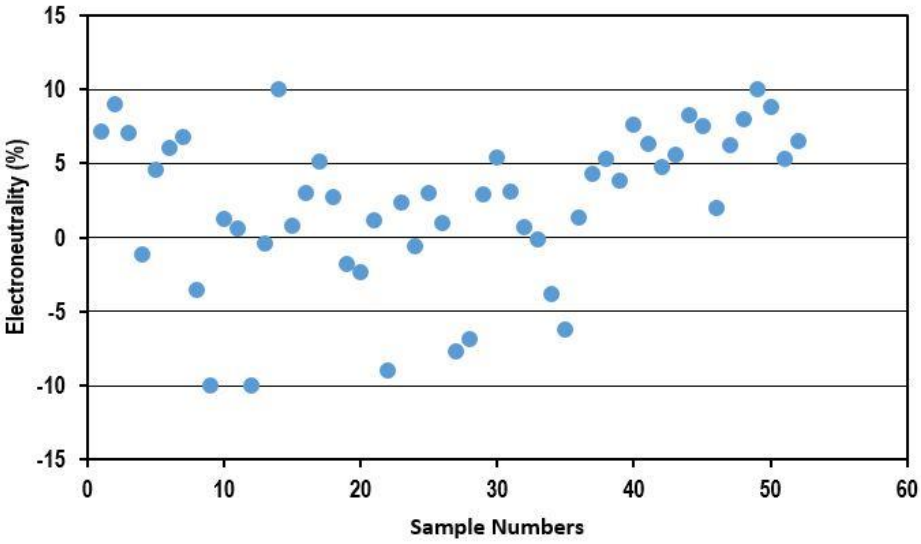

Figure 31 Electroneutrality variation of the groundwater samples

Figure 32 Groundwater sample collection from an operating well and springs

4.1.2 Unsaturated zone sampling

During April 2017 field campaign, calcarenite and paleosols samples were collected from unsaturated zone along a section in Fonte de Areia. The geological sequence in Fonte de Areia consist of carbonate eolianite formation. The consolidated eolianite dunes present in top section of unsaturated zone were formed by wind transported sand from Atlantic during low sea level (personal communication with Joao Silva, 2017). Eolianite dunes are underlain by thick sequence of paleosols. An exposed section of unsaturated zone consisting of both calcarenite and paleosols was selected for sampling. The site may be considered as the representative of the biggest and most important geological formation from groundwater occurrence point of view. Top calcarenite sand and bottom paleosols samples spread across the different vertical depth from the ground surface has been taken for electrical conductivity measurement. Depending on the accessibility along the cliff section, the sampling distance interval has varied in case of calcarenites section, while it was constant in case of paleosols.

First calcarenite sand sample (C1) is from the top of the cliff surface while second (C2) at one meters from the surface. Next sample (C3), has been taken at four meters below the cliff surface due to accessibility limitations. Afterwards, six more sample, each at interval of 20 centimeters were taken. Last calcarenite sample (C9) has been taken from the base of calcarenite sand layer at depth of 5.20 meters from the cliff surface. Between the calcarenite sand and the paleosols, a clear transitional boundary is visible along the bed (Figure 33). Paleosols sampling started from the junction of the calcarenite and paleosols layers, and scoping of paleosols was done with proper attention to prevent least mixing of overlying calcarenite with paleosols sample. A total of nine paleosols samples spread across 1.60 meters vertical distance each at interval of 20 centimeters has been collected. While scoping out the calcarenite and paleosols samples, a few centimeters of the open cliff surface were removed to get the fresh sample (Figure 34) and to avoid any exaggeration of salinity values which might be attributed due to marine aerosol input on open surface.

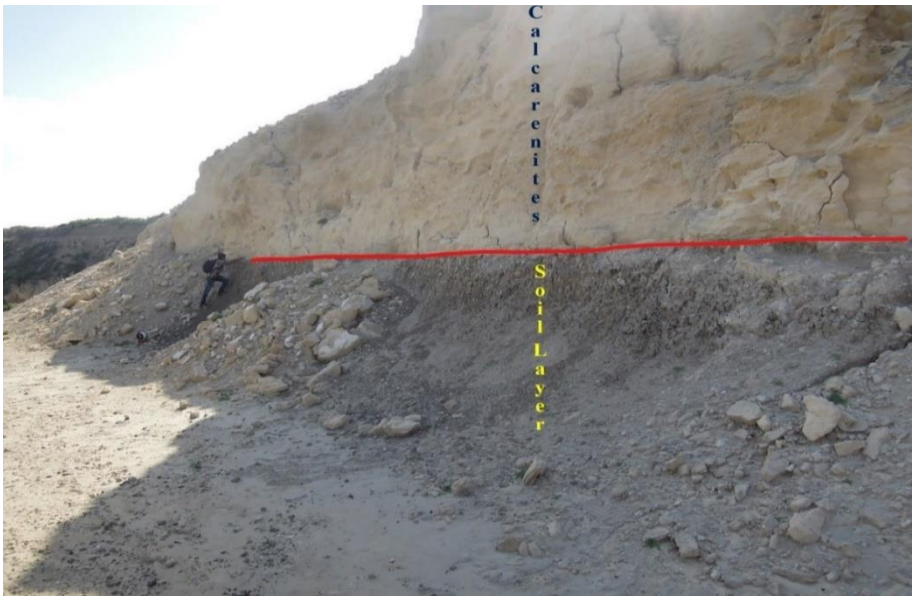

Figure 33 Unsaturated zone cliff section selected for paleosols sampling

Figure 34 Removing the top portion of paleosols to get the fresh samples

The samples collected from field were later analyzed for electrical conductivity determination. 50 grams of each calcarenite sand or paleosols sample were mixed with 250 grams of water having electrical conductivity value of 3 µS/cm. In order to disintegrate the lumps, the solution containing bottle was kept on the electric shaker machine (Figure 35) for 20 hours in addition to manually shaking of bottles at regular interval to avoid any coagulation. Electrical conductivity has been measured at every hour for a continuous period of 20 hours, although the values were stable from 12th hour on wards (Figure 36).

Figure 35 Paleosols samples on the shaker plate for mixing the soluble salts in water

4.2 Unsaturated zone salinity measurements

Plot of electrical conductivity against depth from the surface level shows an elevated concentration close to the surface level, and decreases afterwards (Figure 36). At the surface, the electrical conductivity is lower and increases up to one meter of depth. The area is devoid of vegetation, so enrichment of salts close to a meter depth as most plant species do not take up significant quantities of salts from soil water can't be a factor. The salt accumulation due to evaporation is the most plausible explanation owing to the climatic condition on the island. The electrical conductivity graph after four meters of depth is highly variable. The climatic condition in the form of wet and dry period at the time of sediment deposition may be responsible for the changes in salt concentration. Marine aerosol input aided by dry periods may have increased the salt concentration and vice versa, and is visible through fluctuation in the profile.

Close to five and half meters of depth, where the boundary between calcarenites and paleosols layer is present, the electrical conductivity has increased drastically. Lower permeability of paleosols layers may have trapped the dissolved salt coming with infiltrating rainwater from the top layer and is responsible for increased concentration at the junction layer. After the boundary layer, the electrical conductivity is variable again which may be due to input from marine source and enrichment through climatic drivers.

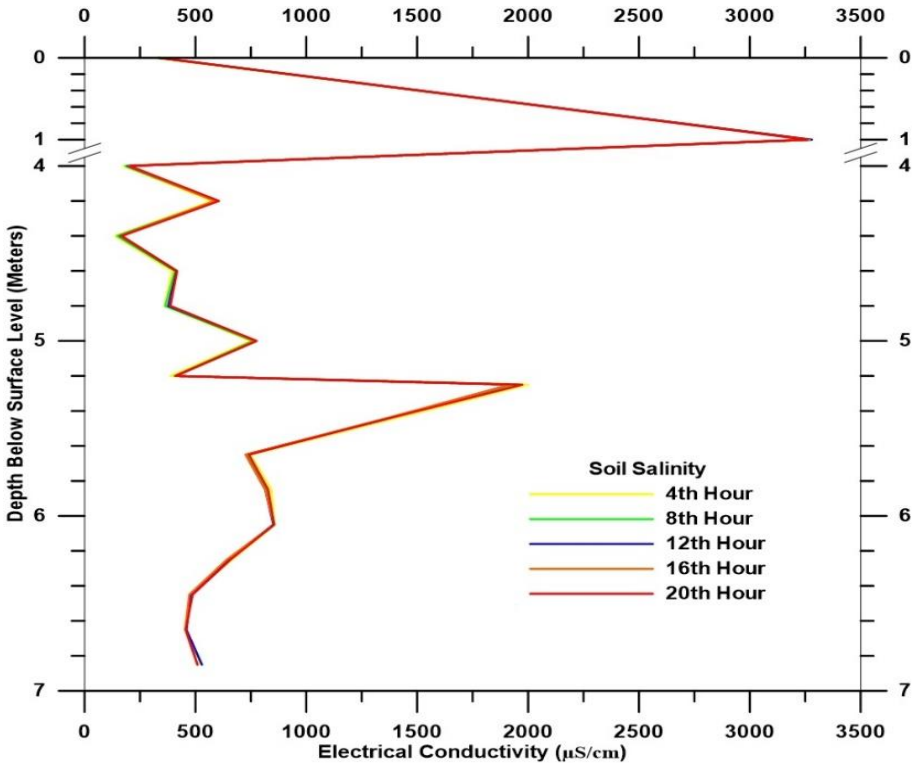

Figure 36 Electrical conductivity of calcarenite sand and paleosols samples

4.3 Groundwater Hydrogeochemical Evolution

Concentration of different major and minor elements, and their interrelationship has been studied to understand and illustrate the hydrogeochemical processes that were involved in different geological formation during the evolution of different groundwater types. Major ion chemistry of groundwater provides basis to investigate the reactions in the subsurface flowing water. How the higher concentration of cations or anions in the groundwater is linked to geological formations, which was further enhanced by evaporation and/or evapotranspiration processes has been studied in detail.

4.3.1 Groundwater Chemistry

The pH varies from 6.6 to 9.2 (Table 4) in all sampling campaigns of 2008 and 2017, the median pH value of 7.8 indicate that most of groundwater samples are alkaline while rest are close to the neutral pH value. The EC varied between 1600 and 6720 µS/cm in February 2008 and from 1920 to 7750 µS/cm in May 2008. For April 2017 sampling, the EC values has been reported between 1486 to 9926 µS/cm (Figure 37). Higher median EC has been found in carbonate eolianite formation as compared to weathered volcanic and hyaloclastite formations indicating major contribution of carbonate minerals in groundwater chemistry in carbonate eolianite formation.

Table 4 Basic statistics of groundwater hydrochemistry

	pH	EC	Na	K	Ca	Mg	Cl	HCO_3	SO_4	NO_3	Br	F	B	Si	As
		µS/cm	mg/L												µg/L
Median	7.8	4149	857	22	17	27	854	597	213	38	3.0	3.0	3.0	19	2.0
Max	9.2	9926	1900	79.4	252	209	2700	1211	529	105.3	8.2	7.9	5.8	46.1	26.0
Min	6.6	1486	174	6.7	4.9	4.5	189	129	26	0.0	0.7	0.0	0.3	3.8	0.0
SD	0.6	1753	386	17.5	42.7	40.3	573	227	116	23.8	1.9	1.4	1.4	10.3	8.0

Groundwater in the Porto Santo vary in their major ion chemistry, with Na as the predominant cation in all the groundwater samples. The concentration of Na varies between 174 to 1900 mg/L (Figure 38) and its median value is 857 mg/L with very minor difference in carbonate eolianite and volcanic formations. Such high concentration of Na in all geological formations point to marine origin of sediments. Submarine and subaerial deposition sequence may have incorporated higher Na in to sediment matrix from the sea water. Only three out of 52 samples have Na concentration less than 200 mg/L, which is higher limit of water consumption according to WHO (2011) standard.

Increase of Na content in makes water unsuitable for agricultural purposes also. Reductions in water infltration can occur when irrigation water contains high Na relative to the Ca and Mg contents. Higher Na causes swelling and dispersion of soil clays, surface crusting and pore plugging. This degraded soil structure condition in turn obstructs infltration and may increase runoff. High Na causes a decrease in the downward movement of water into and through the soil, and actively growing plants roots may not get adequate water, despite pooling of water on the soil surface afer irrigation.

K concentration varies between 6.7 to 79.4 mg/L with median value of 22 mg/L. Highest K concentration has been reported from carbonate eolianite formations. The median concentration value of Ca is 17 mg/L for all sampling site. Carbonate eolianite as well as weathered volcanic have reported highest concentration of Ca. Mg has median concentration of 27 mg/L and with similar values from all kinds of geological formations. Higher concentration of Mg as compared to Ca in groundwater may be due to marine deposition as sea water contains more of Mg than Ca.

Among the anions, Cl has very wide range of concentration (Figure 39). The minimum value is 189 mg/L while maximum is 2700 mg/L with highest standard deviation among all ions. Higher values of Cl have been reported from weathered volcanic, hyaloclastites and carbonate eolianite as well. Highest concentration of Cl ion among all geological formation is indicative of salt incorporation during submarine depositional sequence as sea water contains maximum percentage of Cl. Thirty four of 52 samples have Cl concentration more the maximum allowable limit value of 600 mg/L. WHO has not set any health based guideline value for Cl in drinking water (WHO, 2011).

Although Cl is essential to plants in very low amounts, it can cause toxicity to sensitive crops at high concentrations. Like Na, high Cl concentrations cause more problems in certain kind of crops. Leaf burn of plants is a common symptom of high Cl content in irrigation water. Negative impacts are also reported in citrus fruit trees due to higher Cl content (Richards, 1969).

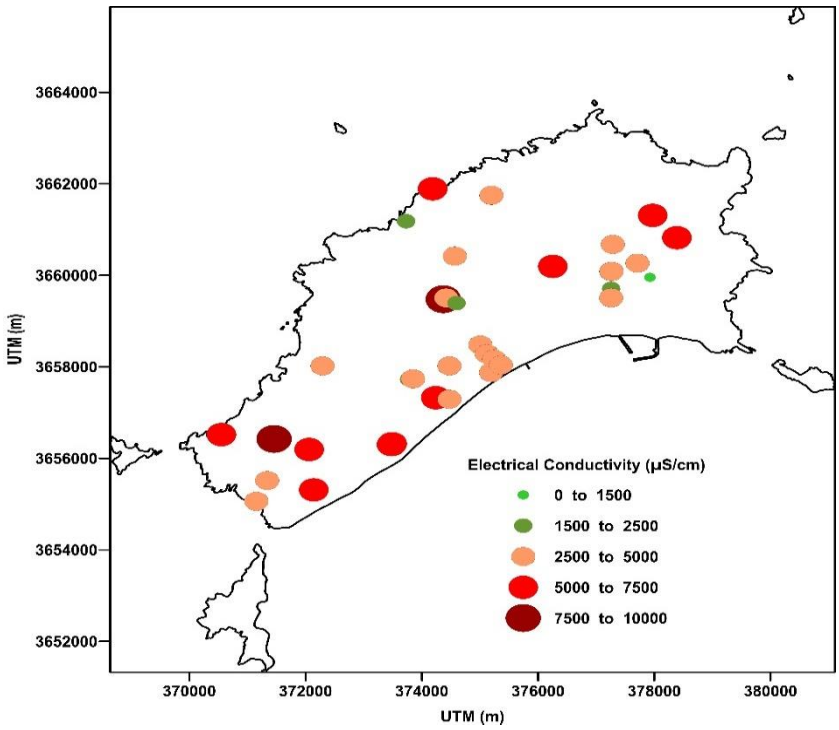

Figure 37 Groundwater electrical conductivity map of Porto Santo

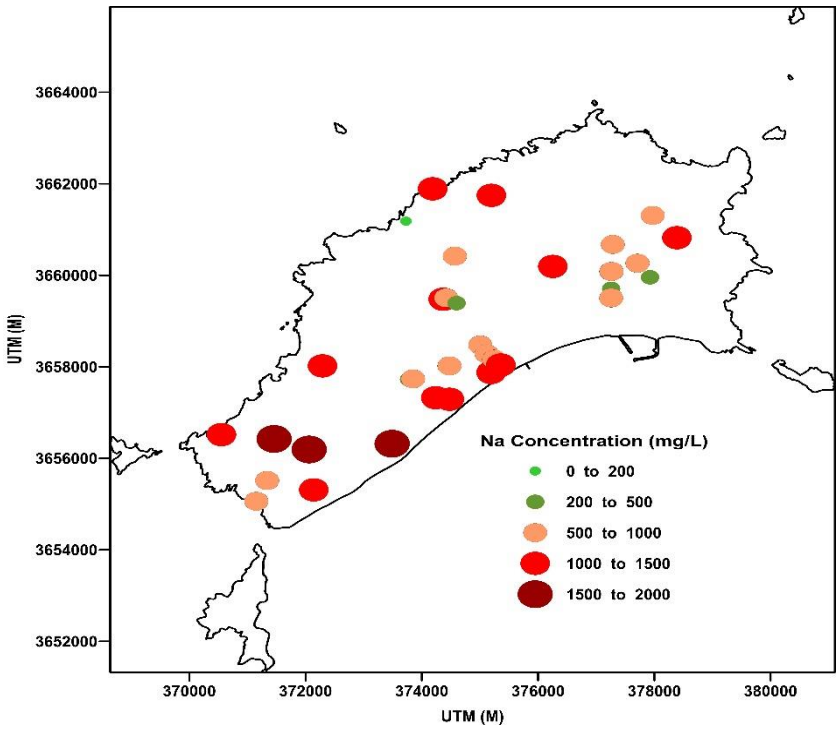

Figure 38 Na concentration (mg/L) map of the study area

HCO_3 presence in the area is marked by higher pH values and corresponds to the carbonate eolianite formation. The median HCO_3 concentration is 597 mg/L. Highest concentration of HCO_3 is from the mine stored groundwater of all geological formation. Long standing time of water in mines may be responsible for higher dissolution of carbonate minerals. No specific correlation of HCO_3 with carbonate eolianite deposit only in the central portion of Porto Santo has been identified (Figure 40).

SO_4 is another anion found in higher concentration in groundwater of Porto Santo. Median concentration of SO_4 is 213 mg/L. Higher concentration are mostly from the wells and mines of carbonate eolianite formation. Higher concentration of SO_4 results in taste impairment of the water. The taste impairment is considered minimal at 250 mg/L and no human health based guideline has been issued with high SO_4 concentration (WHO, 2011). Specific sensitivity of SO_4 has been noticed in plant. High SO_4 has the tendency to restrict the uptake of Ca by plant. Decrease of Ca can result in higher uptake of Na which will result in cationic imbalance in plant (Richards, 1969).

NO_3 concentration in groundwater samples range from zero to 105 mg/L with median value of 38 mg/L. 11 samples have exceeded the desirable limit of 45 mg/L as per WHO standards. The source of nitrogen in groundwater is believed to be derived from biosphere (Saleh, et al., 1999). Nitrogen fixation from the atmosphere aided by soil bacteria helps in ammonium formation. Some local point source injection due to fertilizers, animal excreta and domestic effluents may be responsible for contamination of groundwater at places.

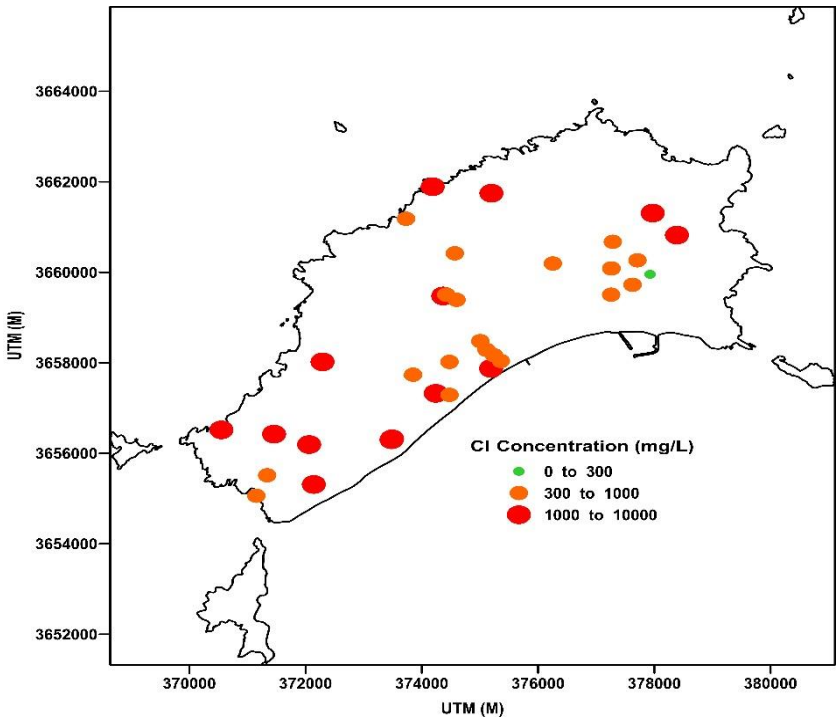

Figure 39 Cl concentration (mg/L) map of the study area

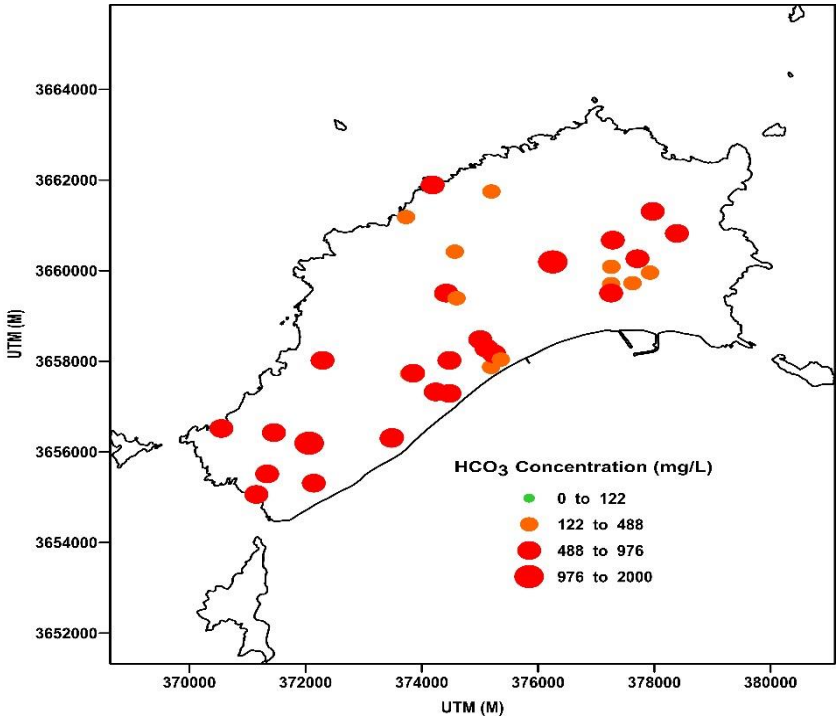

Figure 40 Bicarbonate concentration (mg/L) map of the study area

4.3.2 Ionic dominance

The ionic dominance (mg/L) pattern is in the order of Cl > Na > HCO_3 > SO_4 > Mg > NO_3 > Ca > K (Table 5). Na and Cl are in high concentration among cations and anions, respectively, in the groundwater of the study area. Ionic dominance pattern is same for all three field campaigns. The

groundwater in different geological settings showed occasional different ionic concentrations. In weathered volcanic formations and carbonate eolianite, K was in higher concentration than that of Ca whereas in hyaloclastite, Ca and Mg were in higher concentration than K.

Among anions, HCO_3 exceeds Cl in very few groundwater samples of carbonate eolianite formation. The ionic dominance pattern for the groundwater resembles that of the leachable ions from the soils suggesting of a lithogenic origin of minerals in groundwater and inputs from marine aerosol sources. Slight variation in the ionic dominance pattern in the groundwater of different geological formations is understandable as it is closely related to water rock interaction. Higher concentration of certain ions points to enrichment through evaporation of the preexisting ions in the groundwater.

Table 5 Ionic (mg/L) dominance in different terrains

Terrains	Cations	Anions	Hydrochemical Facies
Carbonate Eolianite	Na > K > Mg > Ca	Cl > HCO_3 > SO_4 > NO_3	Na–Cl–(HCO_3)
Hyaloclastites (Volcanic)	Na > Mg > Ca > K	Cl > HCO_3 > SO_4 > NO_3	Na–Cl–(HCO_3)
Weathered Volcanic	Na > K > Mg > Ca	Cl > HCO_3 > SO_4 > NO_3	Na–Cl–(HCO_3)

4.3.3 Classification of groundwater

The groundwater of all sampling campaigns and geological formations are classified depending upon their ionic strength of select ions. Piper (1944) has proposed categorization of groundwater based on the meq/L percentage content of Na, K, Ca, Mg, Cl, SO_4, CO3 and HCO_3. Distribution of groundwater samples based on the Piper's classification (Figure 41) has indicated that majority of the samples in all sampling campaigns and different geological formations are of Na–Cl–(HCO_3) type. No seasonal and temporal variation in concentrations of these elements for 2008 and 2017 sampling were present.

In cation triangle, a clear pathway towards Na and K is visible indicating enrichment of alkali elements as compared to alkaline earth. Groundwater samples from either geological formation are having lower concentration of rest of the cations. In case of anion triangle, dominance of Cl ion is in most of samples. Carbonate eolianite, volcanic and weathered volcanic are equally following the enrichment of Cl ion. In the diamond section of piper plot, the samples cluster around the saline end. High concentration of dissolved Na and Cl points marine source sediments causing the salinity in the groundwater of the island.

The selected major ions (meq/L) data when plotted in Schoeller (1965) scheme have indicated wide range of concentration in all geological formation. Na has varied between 8 to 83 meq/L, lowest Na content is from the carbonate eolianite samples while highest is from the weathered volcanic formation. Cl concentration among different geological formation has also varied significantly for all sampling sites. The water quality type (Figure 42) is similar in campaigns 2008 and 2017, and can be classified as Na–Cl–(HCO_3).

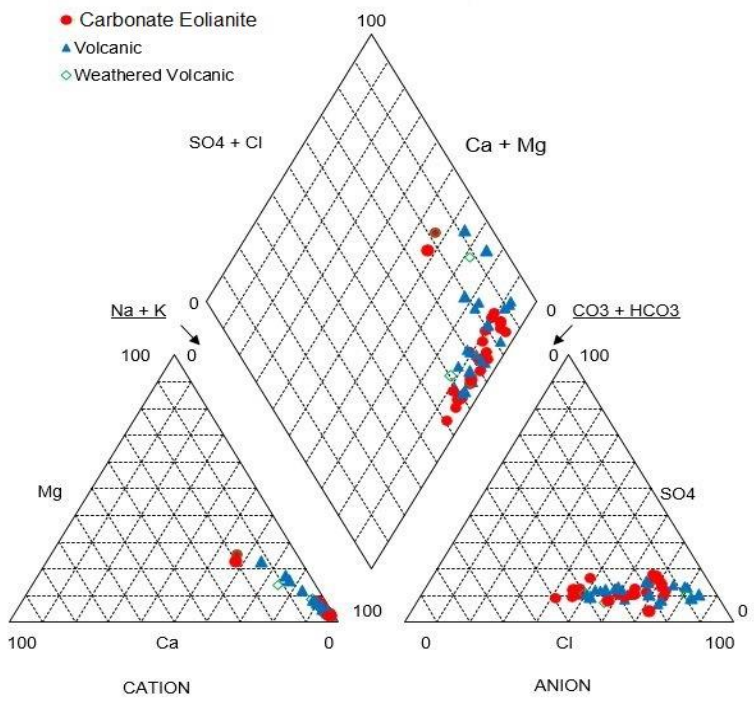

Figure 41 Piper diagram showing groundwater types of the island

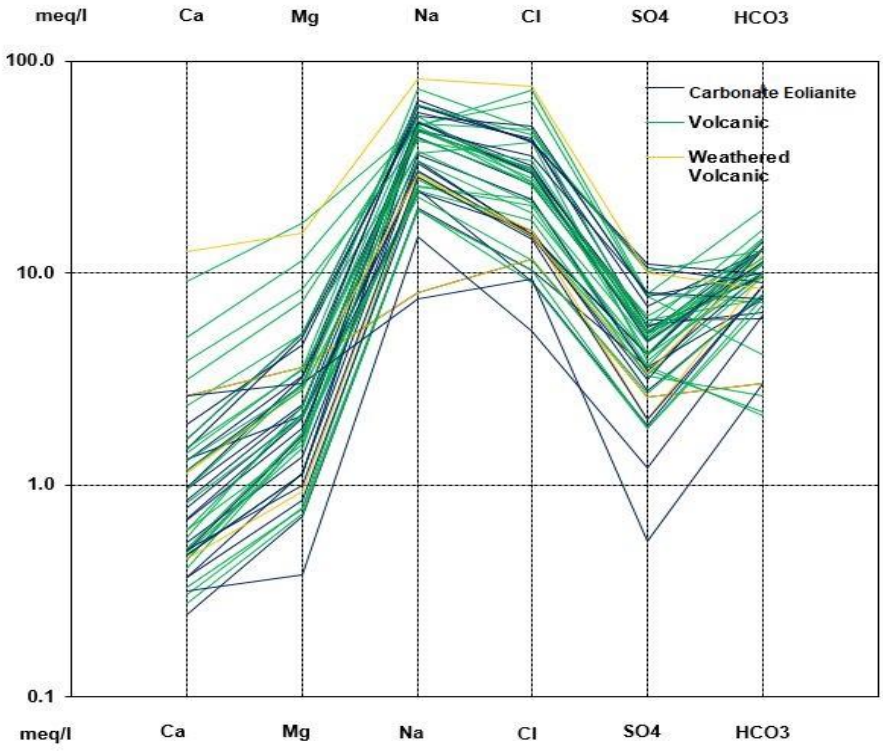

Figure 42 Scholler plot for groundwater samples

4.3.4 Ion exchange indices

The groundwater source can be determined based on meteoric genesis index, which is computed applying Soltan (1999) equation.

$$r_2 = \frac{(K^+ + Na^+) - Cl^-}{SO_4^{2-}} \ (meq/L) \qquad [4]$$

The value of $r_2 < 1$ indicates that the groundwater is of deep meteoric percolation type and $r_2 > 1$ express the water is of shallow meteoric percolation type. The groundwater of different formations of the area is of mixed type, but in general, majority of the analyzed samples shows that it is of shallow meteoric water percolation type (Figure 43). Lower index value is shown by samples from springs and mines, mostly from carbonate eolianite formation which shows that they might have travelled quite long distance before coming out on the surface as spring or getting collected in mines.

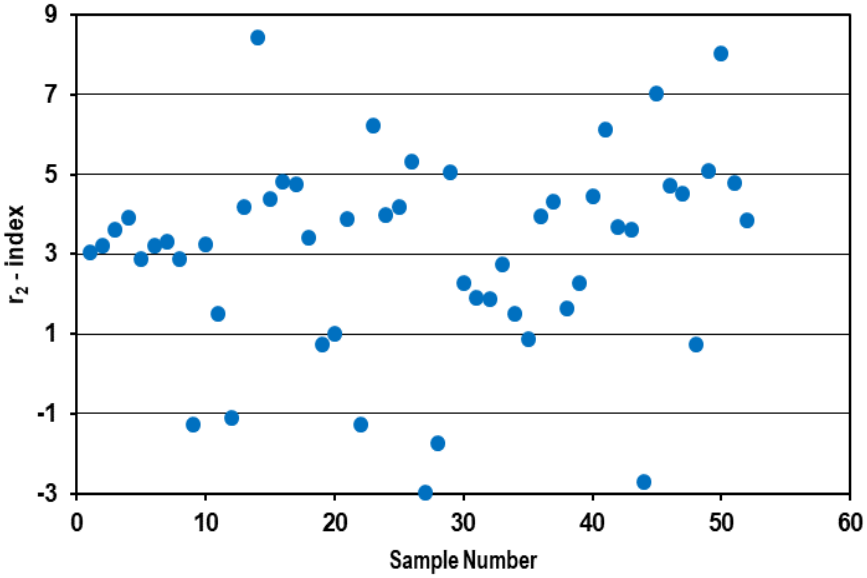

Figure 43 Meteoric genesis Index (r_2)

The role of aquifer material in the evolution of groundwater chemistry can be further examined by determining the chloroalkali index (CAI) for cations (CAI_1) and for anions (CAI_2). It is indispensable to understand the modifications in water chemistry during its movement and residency time for better evaluation of the hydrochemistry of any area more so when different geological formations are present. CAI_1 and CAI_2 equations were developed by Schoeller (1967) to relate the ion exchange process between groundwater and aquifer material. The CAI_1 and CAI_2 are negative (Figure 44) in majority (88%) of the samples indicating the ion exchange between Na–K in water and Ca–Mg in rocks (McIntosh & Walter, 2006).

$$CAI_1 = \frac{[Cl^- - (Na^+ + K^+)]}{Cl^-} \ (meq/L) \qquad [5]$$

$$CAI_2 = \frac{[Cl^- - (Na^+ + K^+)]}{SO_4^{2-} + HCO_3^- + CO_3^{2-} + NO_3^-} \ (meq/L) \qquad [6]$$

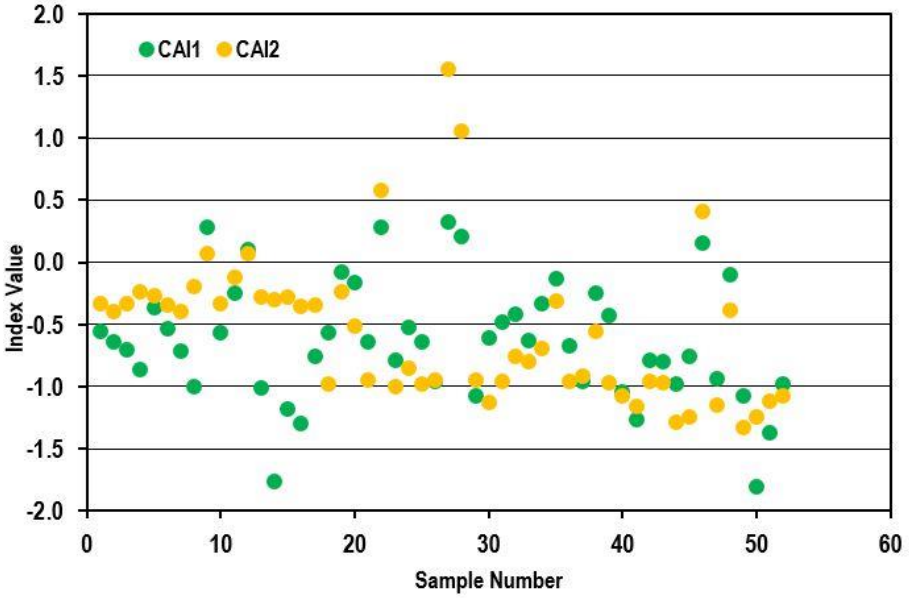

Figure 44 Chloroalkali index for cations and anions

4.3.5 Hydrogeochemical pattern

Na/Cl molar ratio in the groundwater of Porto Santo is 1.17 (Figure 45), which is higher than the typical sea water molar ratio of 0.86 (Moller, 1990). The groundwater molar ratio deviates significantly from the sea water line. The ratio in groundwater was expected to be close to sea water line based on the marine origin of sediments formed either as submarine and subaerial volcanic sequence. Excess source of Na in groundwater is expected to be the result of weathering and dissolution Na containing volcanic rocks. Fine size marine aerosol which shows preferential transport of Na as compared to Cl may be another contributor to excess Na in the groundwater. The contribution of sea salt in salinity increase arising from sea salt spray on small semiarid volcanic islands in Atlantic Ocean has been discussed by (Custodio, 1993; Prada *et al*., 2005).

Br/Cl molar ratio for groundwater samples are 0.0013 which is quite close to the seawater mixing line value of 0.0015 (Francisco & Custodio, 2008) (Figure 46). Br and Cl trapped in the marine sediments coming through either volcanic or wind transport may be responsible for having value close to the sea water line. Br and Cl, owing to its hydrophilic character and small ionic size serve as a natural water tracer close to ideal conservative behavior (Davis, et al., 1998). Neither of the ions have strong affinity for significant ion exchange reactions at low temperatures, nor are they adsorbed onto mineral surfaces, and as they are so highly soluble, which causes less possibility of deviation from natural phase (Cartwright *et al.,* 2006; herczeg *et al,.* 2001).

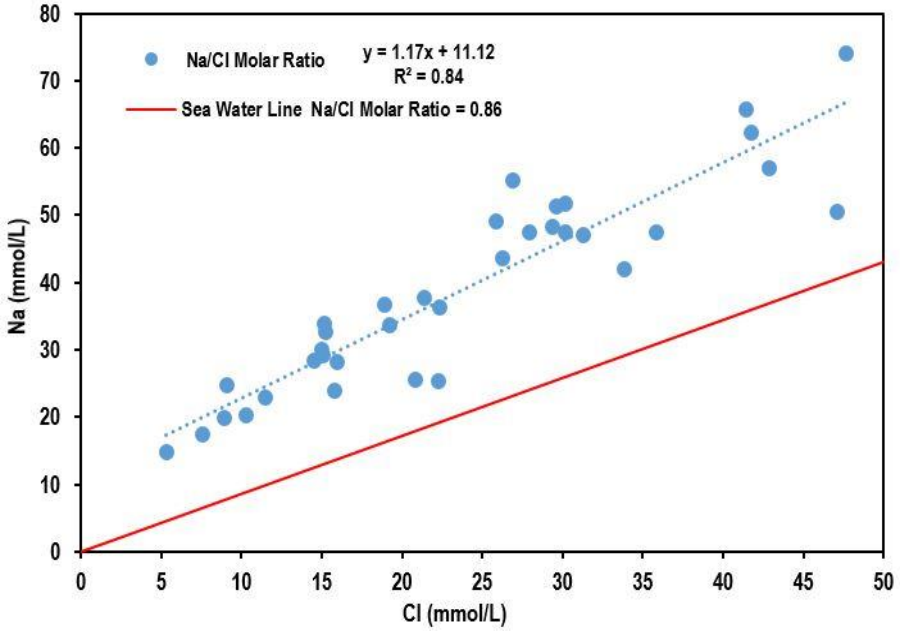

Figure 45 Na/Cl ratio in groundwater of Porto Santo

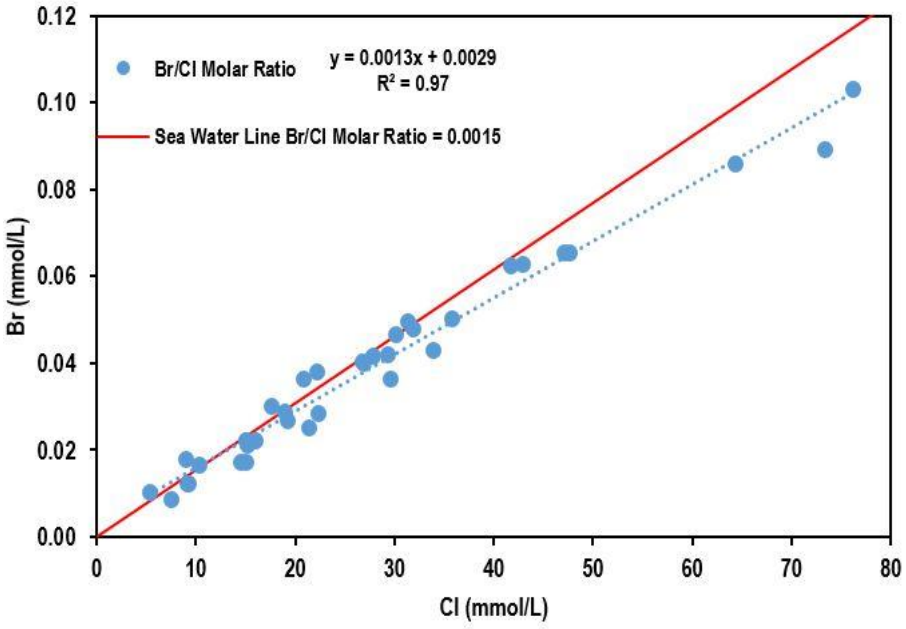

Figure 46 Br/Cl ratio in groundwater of Porto Santo

4.3.6 Minor and trace elements in the groundwater

Groundwater of Porto Santo is enriched in some minor and trace elements also. Some trace elements like Arsenic (As) and Fluoride (F), which possesses health risk to human have elevated concentration in groundwater. Boron (B), although possesses no health hazard to human but can potentially damage plants have high value across the island. Silica (Si) is another minor element which has high concentration in the groundwater of Porto Santo.

Arsenic: Some of the groundwater samples, especially from the carbonate eolianite and hyaloclastic volcanic formation has elevated concentration of As above the permissible limit value of 10 µg/L (Figure 47). The As concentration in unconsolidated formation has been shown to be mostly associated, but not limited to oxidation of arsenical pyrite during groundwater movement (Dhar *et al.,* 1997; Mandal *et al.,* 1998), reductive dissolution of Fe(III) rich oxyhydroxide (Bhattacharya *et al.,* 1997; Nickson *et al.,* 2000; Tossell, 1997) and the desorption of As from aluminosilicate minerals or Al oxides (Frost & Griffin, 1977; Manning & Goldberg, 1997).

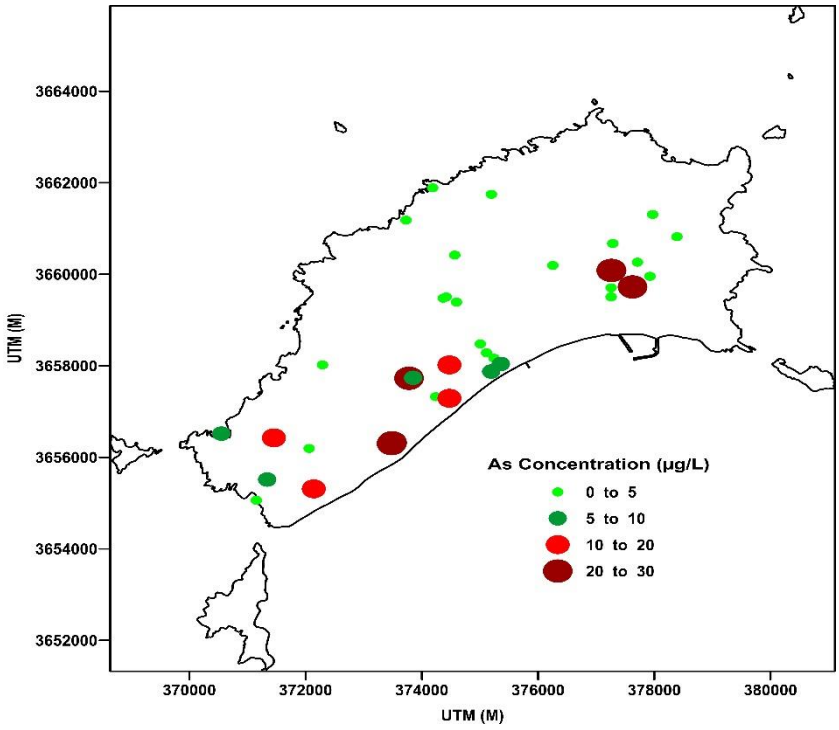

Figure 47 Arsenic concentration in groundwater of the study area

Possible factors controlling the increases in As concentrations in groundwater of Porto Santo appear to be processes associated with neither redox nor dissolution reactions. The absence of correlation between As and SO_4 concentration (Figure 48) and the slightly alkaline pH conditions of the groundwater of Porto Santo rules out oxidation of sulphate bearing minerals as a possible source (Peters *et al.,* 1999; Robertson, 1989; Schreiber *et al.,* 2000). The increased concentrations of As in correlation with HCO_3 rich alkaline groundwater which suggest that HCO_3 competition with $HAsO_4$ is reducing the possible extent of As sorption on Fe and Mn-oxyhydroxides and causing the possible release from the clay materials on the island. Similar study on the releasing of As in Argentina has been carried out by Smedley *et al*., (1998). Hydrothermal activity in hyaloclastic volcanic rocks may be another possible mechanism for As release into the solution phase.

Boron: In natural scenario, B exist in combined form, either as boric acid $[B(OH)_3]$ or borate ions $[B(OH)_4^-]$ in groundwater, especially in regions that are or have been volcanic (Eaton, 1935). In connection with the agricultural significance of this element, it causes injury to plants even when present in smaller concentrations in the soil column. It is desirable for the growth of plant, but the required

concentration is very less and exceedance causes injury (Richards, 1969). The concentration of B in the groundwater of Porto Santo has varied from 0.3 to 5.8 mg/L. Of all the samples, 75% have concentration above 1.5 mg/L which is the upper intake limit of sensitive plants (Figure 49).

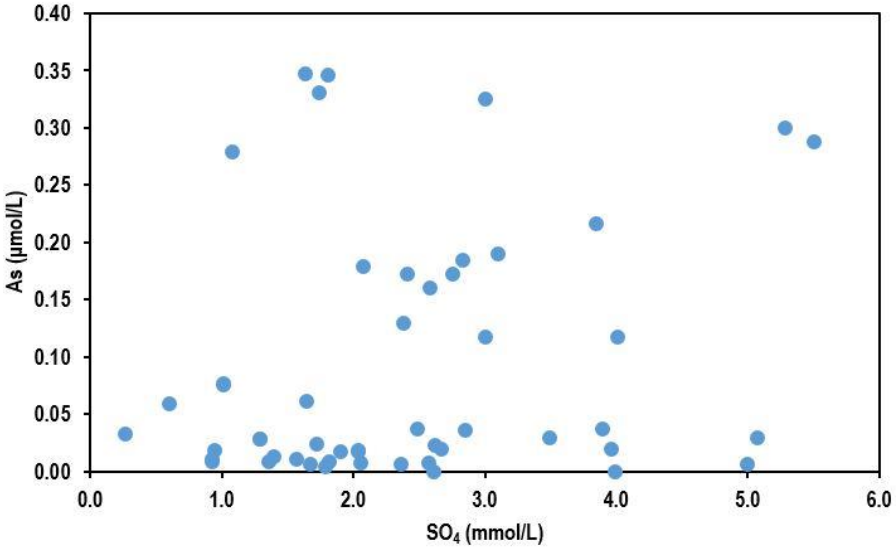

Figure 48 As and SO_4 concentration variation in the groundwater of Porto Santo

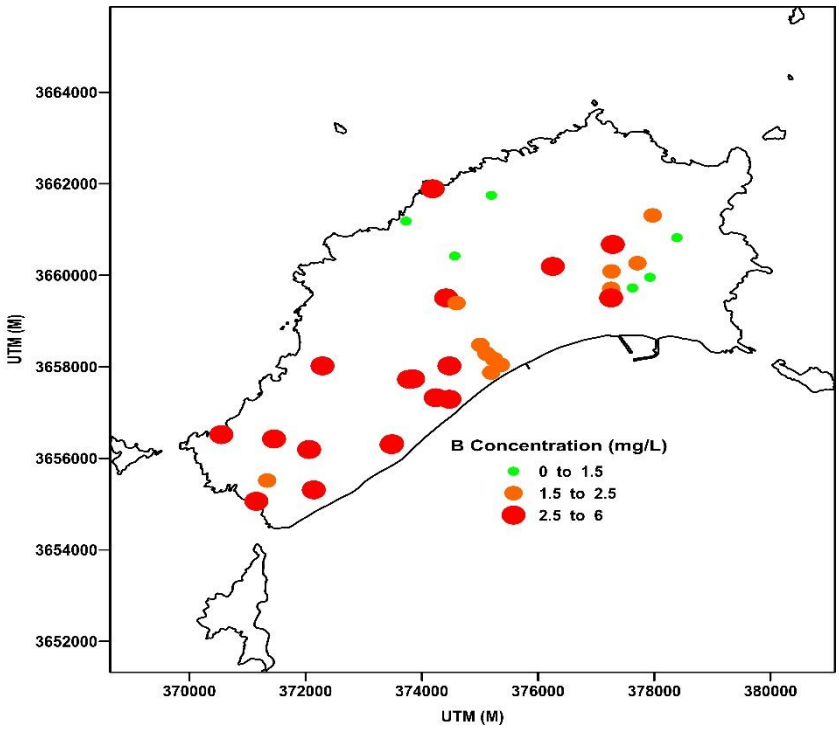

Figure 49 Boron concentration in groundwater of the study area

Fluoride: F occurs as minor element in natural waters, with concentration usually lower than 1 mg/L. In rare geological scenario where aquifers contain F bearing minerals, such as fluorapatite and fluorite groundwater F concentration goes to higher values. Presence of F in groundwater of Porto Santo is associated with fluoapatite and fluorite minerals in the hyaloclastic volcanic rocks aided by alkaline

groundwater which favors the fluoride dissolution. F concentration has varied from 0 to 7.9 mg/L (Figure 50) during all campaigns and is equally high in all geological formations. Only two out of all sampling sites have F concentration less than the WHO permissible limit value of 1.5 mg/L (WHO, 2011). Since Porto Santo island falls in temperate zone where daily water intake is low, concentration up to 2 mg/L is considered as safe limit. Majority of samples have concentration more than 2 mg/L and which points to existing dental fluorosis cases on the island.

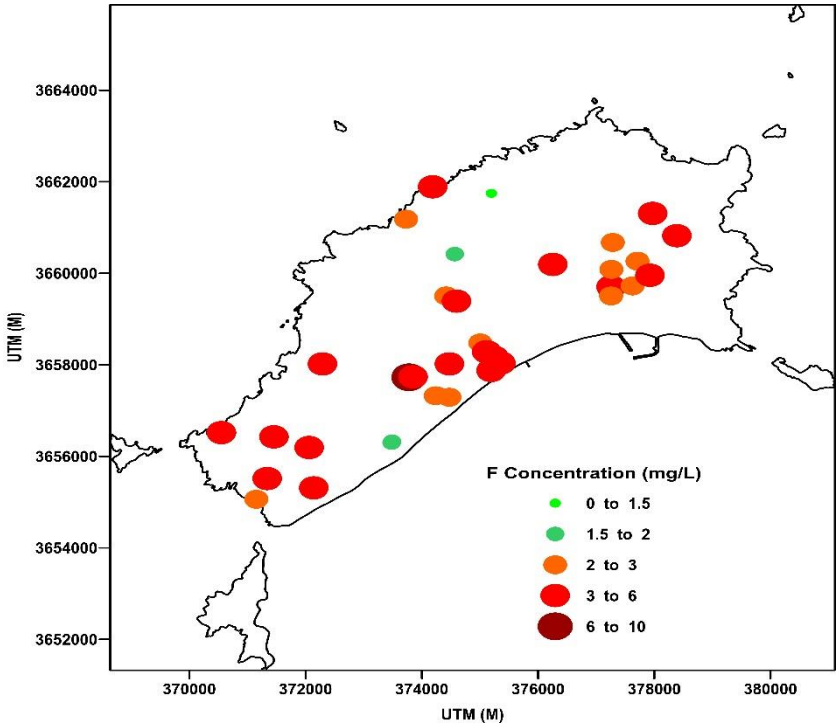

Figure 50 Fluoride concentration in groundwater of the study area

Silica: Si generally account for 5 to 10 % of total dissolved solutes in portable water and < 1% in saline and brines (Davis, 1964). Groundwater analysis often include Si as an easy parameter to measure but its nontoxic nature to humans, animals and plants life has escaped the attentions of hydrochemists (Haines & Lloyd, 1985). Si concentration in groundwater of Porto Santo has varied between 3.8 to 46.1 mg/L (Figure 51), and out of that only 6% of samples have Si content < 10 mg/L. Weathering of volcanic rocks such as trachyte and rhyolite may be responsible for higher Si concentration in the groundwater. Higher temperature during volcanic eruption can triger the melting and dissolution of rocks and may be another possible reason for high concentration in groundwater of Porto Santo.

4.4 Saturation Index

Saturation index (SI) calculates departures from the thermodynamic equilibrium and can be used to trace the path related to the reactivity of minerals in an aquifer. The SI for a particular mineral generally stipulates whether the groundwater is undersaturated (SI < 0), at equilibrium (SI = 0), or supersaturated (SI > 0) with respect to that particular mineral. If groundwater is undersaturated with respect to a mineral, as indicated by a negative SI, the groundwater would theoretically dissolve the mineral if present in the

aquifer matrix. Conversely, if groundwater is supersaturated with respect to a mineral, then the mineral would theoretically precipitate from the groundwater solution phase and will go to the solid phase.

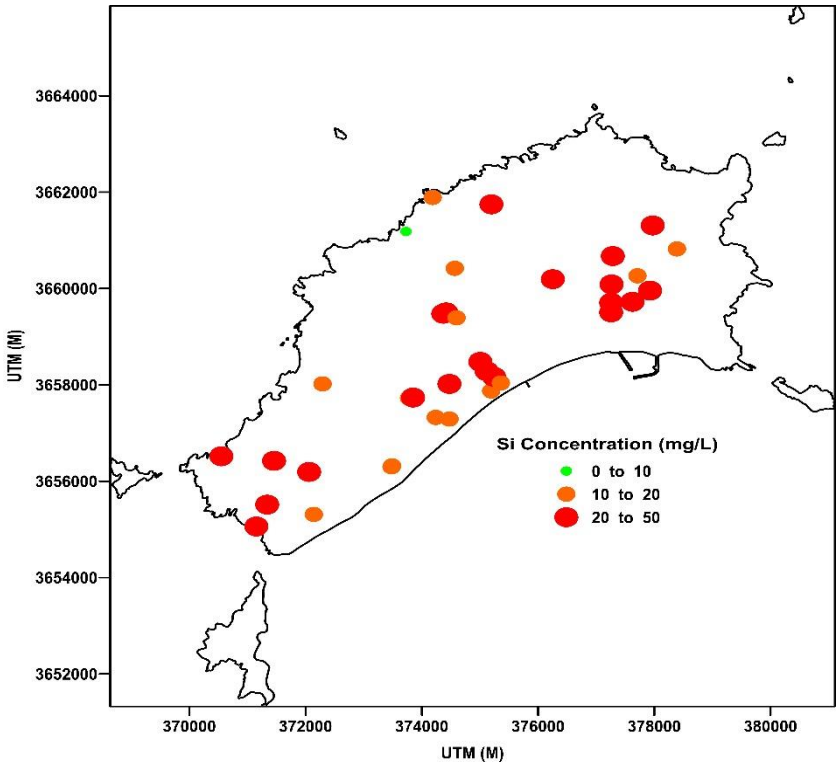

Figure 51 Silica concentration in groundwater of the study area

The geochemical program PHREEQC for Windows has been used to calculate the SI with respect to carbonate, sulphate, halite and siliceous minerals. Calculated SI values (Appendix C) show that groundwater in the Porto Santo is highly undersaturated with respect to halite (NaCl) for all measured samples irrespective of Na and Cl concentration variation. Gypsum is another mineral which shows higher degree of undersaturation after halite. Gypsum undersaturation may be mostly attributed to Ca deficiency because sulphate concentration is high in the groundwater of Porto Santo, and it shows no significant correlation with increasing sulphate concentration (Figure 53). These minerals should, if present, continue to dissolve in the Porto Santo groundwater.

Figure 52 shows that most groundwater sample in the Porto Santo are in equilibrium with respect to aragonite and calcite, and are slightly saturated with respect to dolomite. Saturation with respect to dolomite may be attributed to the higher concentration of Mg as compared to Ca in the groundwater of Porto Santo. Quartz is also showing saturation levels for most of the samples. Saturation of quartz points to the weathering of trachyte and rhyolite rocks.

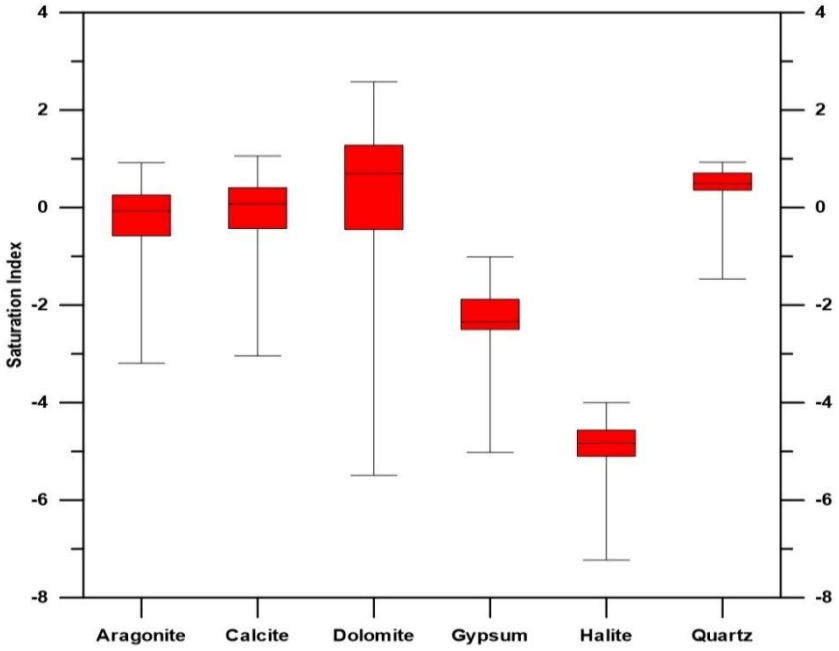

Figure 52 Boxplot showing SI of aragonite, calcite, dolomite, gypsum and quartz in the groundwater of Porto Santo

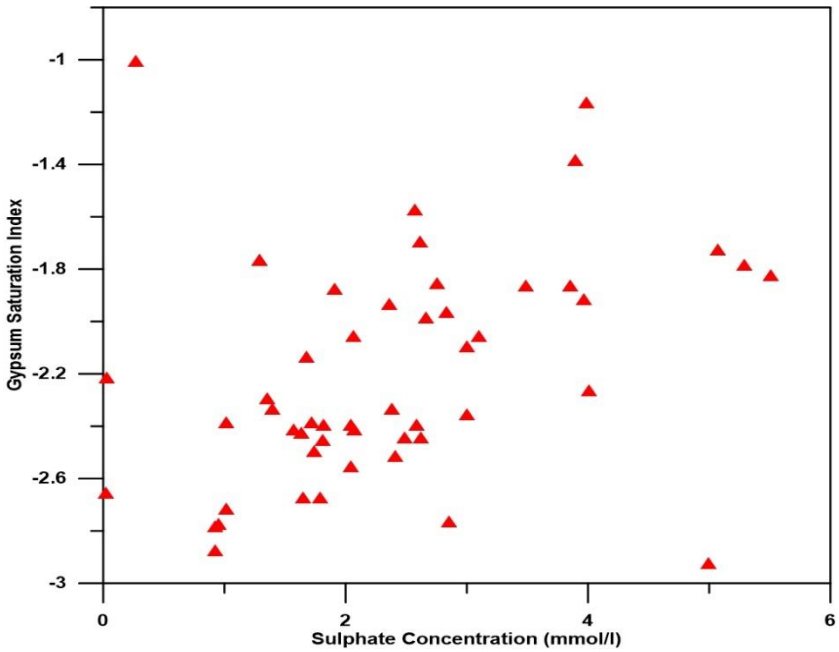

Figure 53 Relation between gypsum saturation index and dissolved sulfate in the Porto Santo groundwater

4.5 Groundwater isotopic signature

The isotopes of oxygen (^{16}O, ^{17}O, and ^{18}O) and hydrogen (^{1}H, ^{2}H, and ^{3}H) are ideal tracers for determining water sources, time scale of movement and mixing because they are integral constituents of water molecules. Stable water isotopes (^{18}O, ^{16}O and ^{2}H) of the island have been studied to validate

the role of evaporation in the geochemical evolution. Based on oceanic proximity of the island, the groundwater isotopic composition is expected to follow the Global Meteoric Water Line (GMWL) (Craig, 1961), while the observed isotopic results of water isotopes deviate significantly from the GMWL slope value of 8 and intercept of 10 (Figure 54) which is produced under equilibrium condensation of rain having 100% humidity. This deviation in isotopic signature of groundwater signify the evaporation effect in the arid climatic condition of the island. This evaporative enrichment of stable water isotopes also points to increased concentration of ions and other salts presents in the groundwater.

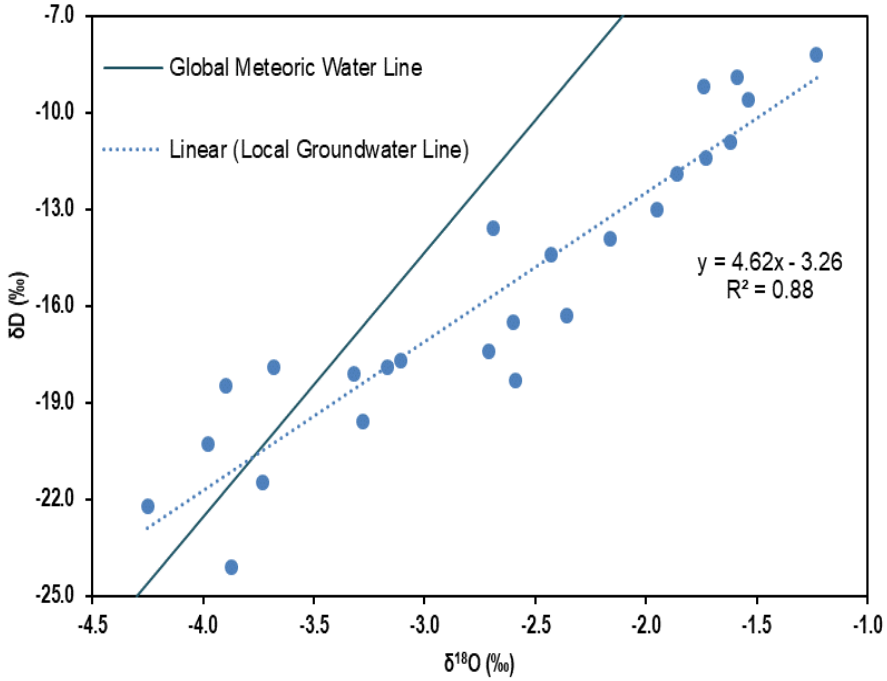

Figure 54 Groundwater stable isotope variation of Porto Santo

Tritium, the radioisotope having half-life of 12.4 years, is ideally suited for studying processes that occur on a time scale of less than 100 years. The radioactive nature and the variation in production over time renders the tritium concentration variable in the hydrosphere and no available standard concentration analogous to V-SMOW for reporting (Kendall & McDonnell, 2012). Tritium measurement of samples ranges between 0.55±0.2 to 1.75±0.2 TU, indicating low residence time of the groundwater.

4.6 Conclusions

The groundwater in Porto Santo island exhibits marginal variations in its chemical parameters between two seasons of 2008 and up to 2017. Higher electrical conductivity measurements from carbonate eolianite, paleosols and groundwater samples points to high base line salinity in the geological formation. Na among cations and Cl among anions are dominant ions in the groundwater, and there is no temporal change in ionic dominance. High Na and Cl content could be due to the dissolution of salts in the aquifer material which was further enhanced by evapotranspiration and marine aerosol spraying. Carbonate rock dissolution may have been responsible for Mg-Ca contribution and ion exchange process for higher HCO_3–SO_4 content in the groundwater. The groundwater is of Na–Cl–HCO_3^- types and no change has been noticed in groundwater types in measured spatial and temporal domain. Ion

exchange index showed that majority of groundwater is of shallow meteoric percolation type. Also, significant exchange between Na and K of groundwater with Ca and Mg of aquifer has been shown by CAI measurements. Supersaturation of Si reveals weathering of silicate rocks while dolomite precipitation is favored by higher Mg concentration. The groundwater chemistry is influenced by water–rock interaction, aquifer material mineralogy and sea spray input, whereas the aquifer hydraulics play limited role in hydrogeochemical processes.

CHAPTER

5

Conclusions and Recommendations

The groundwater of Porto Santo has been the subject of detailed hydrochemical and hydrogeological studies during the present investigation. These studies imparted a broad knowledge of major aquifers and it's physical and chemical properties. A summary of the main conclusions of the present investigation are presented in the following paragraphs:

1. Porto Santo has been roughly classified into four aquifers based on different geological formations. Carbonate eolianite formation in central portion is the principal and most productive aquifer from the island's perspective. Beach sands formation in the eastern and southeastern portion is another low thickness aquifer. Volcanic and weathered volcanic aquifers transmit water through fractures and fissures but the clay filling in fractures constitute a limitation to groundwater flow.

2. Groundwater discharge from Porto Santo island is essentially by three ways: (1) water pumped from boreholes or wells drilled in to the aquifers; (2) water tapped at discharge points of springs and mines; and, (3) the possible submarine groundwater discharge to the sea. Due to the lack of data, no volumetric budget of groundwater discharge through either means is available.

3. The island receives an average annual rainfall of 457 mm mostly during winter months in the form of high rainfall events which mostly goes as runoff. The potential evapotranspiration calculated using Thornwaithe, Pan evaporation and Penman methods shows that potential evapotranspiration on the island is 1.9 to 4.1 times of the average annual precipitation depending on the method. Groundwater recharge estimation through soil water budget methods yields no recharge amount on the island. Overestimation of evapotranspiration may have cause the inaccuracy in recharge measurement. Geochemical chloride mass balance method gives recharge value of 11.4 mm per year. Heavy rainfall in short duration generates high runoff on the island. Prevailing aridity on the island is implicit through water loss through runoff and evapotranspiration.

4. The water table elevation measurement shows that natural groundwater flow follows topography. The carbonate eolianite formation acts as discharge zone by receiving groundwater from high elevation area located in north and south of the island. Beach sands formation located in east and south east has the lowest water head on the island. Lower hydraulic head near coast point to higher probability of sea water intrusion because of groundwater abstraction for irrigation.

5. Carbonate eolianite formation have natural background salinity. Genesis of high salinity Porto Santo rocks may be related to both submarine and subaerial nature of volcanism. Volcanic rocks formed within the sea may have trapped the salts present in sea water at the time of their deposition. Salt

deposition from the atmospheric input is the form of wet and dry deposition is another contributor to the island. Presence of high salinity at shallow depth in paleosols profile indicates the role of evaporation in enriching the salt concentration. Salinity fluctuation at depth in paleosols profile may be either due to variation in atmospheric input at the time of their deposition or due to washing away of salt with percolating rain water through the geological layers.

6. Origin of high salinity in the groundwater of Porto Santo aquifers has been confirmed with different hydrogeochemical processes. The groundwater of Porto Santo is slightly alkaline irrespective of the nature of geological formation. An average temperature value of 20.7 °C has been recorded of the groundwater samples. Groundwater electrical conductivity is equally high in all major formations of the island. Along the coast, a mix of high and mid-range conductive groundwater has been found. Cl is the most dominant ion in majority of groundwater samples, while Na is dominant cation. Cl has dominated the groundwater chemistry even in carbonate eolianite deposits due to higher solubility of Cl minerals as compared to calcite or dolomite. Highest HCO_3 concentration from the mine water indicates the long residence time of water has dissolved more of carbonates. Groundwater type is Na–Cl–(HCO_3) in all major aquifers irrespective of sampling years.

7. Ionic ratio proves that evolution of groundwater towards Na-Cl-HCO_3 is not only dominated by source rock dissolution, but marine aerosol is also contributing significantly in to it. Na/Cl and Br/Cl signatures of marine water is identifiable in groundwater of Porto Santo.

8. Groundwater of Porto Santo is enriched in minor ions like As, B, F and Si. As mobility in groundwater on the island is related to hydrothermal sources in hyaloclastic rocks and higher concentration of HCO_3, which causes release of As from clay minerals. Volcanic rocks are the main source of B while fluorapatite and fluorite minerals in hyaloclastic rocks causes higher concentration of F in the groundwater. Si presence in higher concentration is related to presence of trachyte and rhyolite volcanic rocks on the island.

9. Speciation estimates for the aquifer suggest that only a few minerals are at saturation level in the groundwater. Groundwater samples from carbonate eolianite formation are either in equilibrium or saturated with respect to aragonite, calcite and dolomite. Gypsum and halite are undersaturated in all samples of carbonate eolianite. Volcanic hyaloclastite formation has mixed pattern for aragonite, calcite and dolomite, indicating carbonate intercalation at places. Si is in equilibrium or at saturation level across all geological formation.

10. Stable isotopes of groundwater are considered as a proxy to know the evaporation effect. Significant deviation in local groundwater line from global meteoric water line confirms the dominance of evaporation in increasing the salt concentration in the soil and the groundwater. Lower tritium value measurements from the groundwater terms it as young water formed after nuclear testing decade of 1960s.

5.1 Recommendations

High baseline salinity in the groundwater of Porto Santo makes it unsuitable for various domestic and agricultural uses. Domestic supply is provided after desalinization which may be associated with certain costs. Agricultural, gardening and other small demands are still met through pumping of high saline groundwater. High electrical conductivity and elevated concentration of Na, Cl, SO_4, and B makes the water unfit for agriculture and gardening use. Keeping in view the demand and small population size of permanent residents of Porto Santo rain water harvesting could prove to be an ideal option for storing the rain water using that for small scale indoor and outdoor use.

5.1.1 Water Conservation Practice

Rain water harvesting (RWH) is the technique of collection, filtration and storage of rain water from roof tops, paved and unpaved areas for multiple use at surface, subsurface artificial structures and in subsurface aquifers, before it is lost as surface run-off. The augmented resource can be harvested in the time of need. The need of RWH practice is needed on the island due to following:

- To overcome the inadequacy of water to meet the demands,
- To minimize groundwater decline,
- To minimize the surface runoff during high rainfall event,
- To minimize the use of high salinity water for daily and agricultural use.

The advantages associated with the RWH practice includes:

- Stored water is not directly exposed to evaporation and pollution,
- No land is wasted for storage purpose and no population displacement is involved,
- Storing water underground is environment friendly,
- Cost associated with the construction of the RWH structures are not high,
- Mitigates the effects of drought.

Since major parts of the houses and roads are under the roofs or covered under the impervious material, the RWH practice could be ideal for the island. Harvested rainwater can be stored in the tank (Figure 55), and can be used for non-potable purposes such as garden use, toilet flushing, washing clothes and in the hot water systems. This may constitute more than three-fourth of the water consumed within the island. Long season crops like pomegranate, grapes, vegetables, cut flowers, and to a lesser extent citrus fruits grown on the island can also be watered through tank storage.

The mean annual rainfall is less than 500 mm, with October and November being the wettest month of the year, while July and August, the driest month. Other than rainfall that influences the decision of rainwater harvesting are the extent of connected roofs and the type of end use planned for the water. Estimation of rainwater tank capacity depends on simple water balance model. The volume of rainwater storage in the tank depends on the input volume in the tank and the demand met from the rainwater as an alternative water source for the selected use. The storage level in the tank would depend up on the rainfall frequency and amount, and the end use. Individual potential tank user should predetermine the

planned demand on the tank: external (garden and small croplands) or internal use (toilets only, laundry only or the combination of the above) and the desired level of reliability prior to selecting the appropriate size. In order to avoid wastage of water through evaporation, the tank should be closed. Other important components of the RWH structures includes first rain separator, filter unit, delivery system, outlet to sewage during spill over situations and usage.

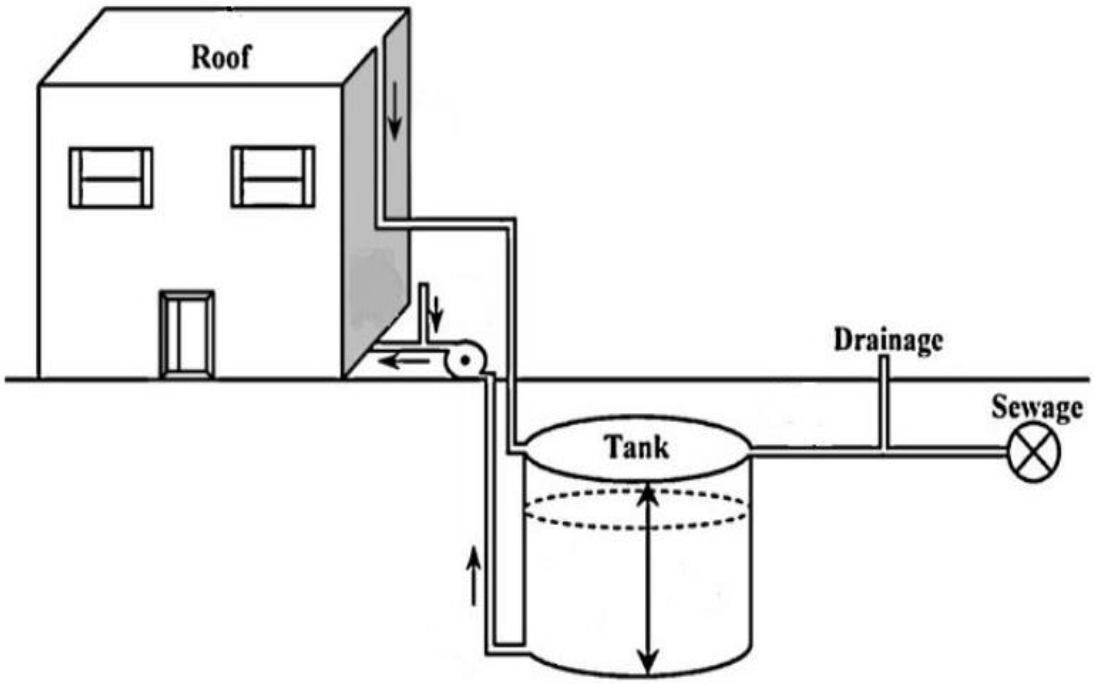

Figure 55 Schematic view of rain water harvesting system

Runoff from the roof for RWH practice is given preference over surface catchment area owing to its relatively unpolluted nature and makes it most appropriate source for water collection (Förster, 1999; Farreny *et al.,* 2011). Water quality of rooftop runoff also varies on roof type and the environmental conditions, including local climate and atmospheric pollution. To have better insight about the water quality of the runoff collected at different roof types viz. flat gravel (FG), clay tiles (CT), metal and plastic roofs, Farreny *et al.,* (2011) has studied the water quality results of the runoff collected in the UAB University Campus, in Cerdanyola del Valle`s (metropolitan region of Barcelona, NE Spain). The study concentrated mailnly on selected quality parameters : pH, EC, Total Suspended Solids, Total Organic Carbon, SO_4, NO_3, NH_4 and total carbonate system (HCO_3, CO_3 and H_2CO_3). Flat gravel roofs encompasses highest pollution level of all roof types selected for the study. Weathering of gravel from the roof surface and the accumulated deposits of particulates and associated flora was the plausible explanation for the elevated pollution level from flat gravel roof runoff. Sloping roofs, on the other hand, avoid the long standing water column over it's surface which prevents the development and growth of mosses, algal crust, lichens, etc.

Due to limited number of vehicles and absence of industry, rain water quality degradation from chemical contaminants arising from traffic and industrial pollution is not a case on the island and thus is a

advantageous thing. A practical implementation of RWH strategy would divert the dirty runoff from the first few millimeters of the initial discharge from the roof surface, which is generally of poor quality due to accumulation of dust, sediments, bird and animal droppings, and leaves and debris from the surrounding areas (Villarreal & Dixon, 2005). It is necessary to initially waste a fixed portion of rainfall from a storm event through first rain separator to improve water quality. This water is called the first flush containing large amount of dust, animal droppings and debris (Yaziz *et al.,* 1989; Jenkins & Pearson, 1978).

The interior of the water storage tanks should be cleaned regularly to remove dust and debris so as to maintain the quality of collected rainwater as high as possible. The advisable season for this to be done is just before the first rainfall events. Chlorination practice is one common disinfection strategies should be applied to the stored rainwater to improve its microbiological quality.

Island dwellers can use rainwater for toilet flushing or watering the garden or crops because it is available for free and its use reduces their expenses for desalinized drinking water that they obtain from drinking water companies. When intended for drinking purposes, stored rainwater should be treated such that drinking water quality is obtained, the efficacy of treatment depending on the level of contamination. Presence of microbial indicator is another quality parameter to looked upon in collected rainwater, if drinking demands are to be met. However, for other domestic purposes, such as toilet flushing, watering indoor plants or ornamental garden plants and cleaning floors, proper preventive and maintenance procedures may guard the microbiological quality and safe use of stored rainwater.

CHAPTER

6

References

Allison, G. A. & Hughes, M. W., 1978. The use of environmental chloride and tritium to estimate total recharge to an unconfined aquifer. *Aust. J. Soil. Res., 16,* pp. 181-195.

Antunes, S. C. et al., 2008. Spatial and temporal distribution of litter arthropods in different vegetation covers of Porto Santo Island (Madeira Archipelago, Portugal). *European journal of soil biology,* 44(1), pp. 45-56.

Bhattacharya, P., Chatterjee, D. & Jacks, G., 1997. Occurrence of Arsenic-contaminatedGroundwater in Alluvial Aquifers from Delta Plains, Eastern India: Options for Safe Drinking Water Supply. *International Journal of Water Resources Development, 13(1),* pp. 79-92.

Blanchard, D. C., 1985. The oceanic production of atmospheric sea salt. *Journal of Geophysical Research: Oceans, 90(C1),* pp. 961-963.

Bonython, C. W., 1956. The salt of Lake Eyre – its occurrence in Madigan Gulf and its possible origin. *Royal Society of South Australia Transactions, 79,* pp. 66-90.

Cachão, M., Rodrigues, D. & Marques DA Silva, C., 2003. *Geological evolution and paleoenvironments of Madeira and Porto Santo islands.* Madeira, Island Ecosystems Conservation and Molecular Approach, University of Madeira.

Cachão, M., Rodrigues, D., Marques DA Silva, C. & Mata, J., 1998. *Biostratigraphia (Nanofosseis calcarios)ne interpretacao paleoambiental do Neogenico de Porto Santo (Madeira).* s.l., Actas V Cong. Nac. Geologia, Com. Inst. Geol. Mineiro 84 (1), A185-A188.

Cartwright, I., Weaver, T. R. & Fifield, L. K., 2006. Cl/Br ratios and environmental isotopes as indicators of recharge variability and groundwater flow: an example from the southeast Murray Basin, Australia. *Chemical Geology, 231(1),* pp. 38-56.

Chivas, A. R. et al., 1991. Isotopic constraints on the origin of salts in Australian playas. 1. Sulphur. *Palaeogeography, Palaeoclimatology, Palaeoecology, 84(1-4),* pp. 309-332.

Condesso de Melo, M. et al., 2008. *Use of Geochemical Tools to Study Groundwater Salinization in Volcanic Islands: a Case Study in the Porto Santo (Portugal) and Santiago (Cape Verde) Islands.* Naples, Florida, s.n., pp. 41-44.

Cook, J. M., Edmunds, W. M. & Robins, N. S., 1991. Groundwater contribution to an acid upland lake (Loch Fleet, Scotland) and the possibilities for amelioration. *Journal of Hydrology, 125(1-2),* pp. 111-128.

Cooper, A. H., 2002. Halite karst geohazards (natural and man-made) in the United Kingdom. *Environmental Geology 42,* p. 505–512.

Cordeiro, N., Silva, J., Gomes, C. & Rocha, F., 2010. Bentonite from Porto Santo Island, Madeira archipelago: surface properties studied by inverse gas chromatography. *Clay Minerals,* Volume 45, p. 77–86.

Craig, H., 1961. Isotopic variations in meteoric waters. *Science, 133(3465),* pp. 1702-1703.

Custodio, E., 1993. *Coastal aquifer salinization as a consequence of aridity: the case of Amurga Phonolitic massif, Gran Canaria Island.* Barcelona, CIMNE, Barcelona, pp. 81-98.

Datta, P. S., Bhattacharya, S. K. & Tyagi, S. K., 1996. 18O studies on recharge of phreatic aquifers and groundwater flow-paths of mixing in Delhi area. *Journal of Hydrology 176,* p. 25–36.

Davis, S. N., 1964. Silica in streams and groundwater. *Americal Journal of Science, volume 262,* pp. 870-891.

Davis, S. N., Whittemore, D. O. & Fabryka-Martin, J., 1998. Use of chloride/bromide ratios in studies of portable water. *Ground Water, 36(2),* pp. 338-350.

Dhar, R. et al., 1997. Groundwater arsenic calamity in Bangladesh. *Current Science,* pp. 48-59.

Duarte, R. S. E. S. M., 1988. *Captações de Águas Subterrâneas na Ribeira de Machico.* Lisboa, Simpósios de Geologia Aplicada e do Ambiente: V-Hidrogeologia das Rochas Vulcânicas. Dep. Geol. Univ. Lisboa, pp. 55-62.

Eaton, F. M., 1935. Boron in soils and irrigation waters and its effect on plants, with particular reference to the San Joaquin Valley of California. *United States Department of Agriculture, Economic Research Service, Technical Bulletin No. 448*, February.

Erickson, D. J. & Duce, R. A., 1988. On the global flux of atmospheric sea salt. *Journal of Geophysical Research: Oceans, 93(C11),* pp. 14079-14088.

Eriksson, E. & Khunakasem, V., 1969. Chloride concentration in groundwater, recharge rate and rate of deposition of chloride in the Israel Coastal Plain. *Journal of Hydrology, 7,* pp. 178-197.

Farreny, R. et al., 2011. Roof selection for rainwater harvesting: quantity and quality assessments in Spain. *Water research, 45(10),* pp. 3245-3254.

Feraud, G. et al., 1981. New K-Ar ages, chemical analyses and magnetic data of rocks from the islands of santa maria (azores), porto santo and madeira (madeira archipelago) and gran canaria (Canary Islands). *Bulletin of Volcanology, Volume 44, Issue 3,* p. 359–375.

Ferguson, G. & Gleeson, T., 2012. Vulnerability of coastal aquifers to groundwater use and climate change. *Nature Climate Change, 2(5),* pp. 342-345.

Ferreira, M. P., Macedo, C. R. & Ferreira, J. F., 1988. *K-Ar Geochronology in the Selvagens, Porto Santo and Madeira Islands (Eastern Central Atlantic): A 30 m.y. Spectrum of Submarine and Subaerial Volcanism.* s.l., Lunar and Planetary Science Conference, volume 19.

Ferreira, M. P. & Neiva, C., 1996. *Carta Geologica de Portugal, Folha de Ilha de Porto Santo,* Coimbra: Universidade de Coimbra/ Instituto Geologico e Mineiro.

Fisher, R. V. & Schmincke, H. U., 1984. Alteration of volcanic glass. In: *Pyroclastic Rocks.* Berlin Heidelberg: Springer, pp. 312-345.

Förster, J., 1999. Variability of roof runoff quality. *Water Science and Technology, 39(5),* pp. 137-144.

Francisco, J. A. & Custodio, E., 2008. Using the Cl/Br ratio as a tracer to identify the origin of salinity in aquifers in Spain and Portugal. *Journal of Hydrology,* Volume 359, p. 189– 207.

Frost, R. R. & Griffin, R. A., 1977. Effect of pH on adsorption of arsenic and selenium from landfill leachate by clay minerals. *Soil Science Society of America Journal, 41(1),* pp. 53-57.

Fuentes, E. et al., 2010. Laboratory-generated primary marine aerosol via bubble-bursting and atomization. *Atmospheric Measurement Techniques, 3(1),* pp. 141-162.

Gilfedder, M., Mein, R. G. & Connell, L. D., 2000. Border Irrigation Field Experiment. II: Salt Transport. *Journal of Irrigation and Drainage 126,* p. 92–97.

Gonfiantini, R., 1978. Standards for stable isotope measurements in natural compounds. *Nature 271,* p. 534–536.

Gong, S. L., Barrie, L. A. & Lazare, M., 2002. Canadian Aerosol Module (CAM): A size-segregated simulation of atmospheric aerosol processes for climate and air quality models 2. Global sea-salt aerosol and its budgets. *Journal of Geophysical Research: Atmospheres, 107(D24),* pp. AAC 13-1.

Grindley, J., 1967. The estimation of soil moisture deficit. *Meteorological Magazine 96 (1137),* pp. 97-108.

Grindley, J., 1969. *The calculation of actual evaporation and soil moisture deficits over specified catchment areas.* s.l., Meteorological Office Bracknell.

Haines, T. S. & Lloyd, J. W., 1985. Controls on silica in groundwater environments in the United Kingdom. *Journal of Hydrology,* Volume 81, pp. 277-295.

herczeg, A. L., Dogramaci, S. S. & Leaney, F. W., 2001. Origin of dissolved salts in large, semi-arid groundwater system: Murray Basin, Australia. *Marine and Freshwater Research, 52(1),* pp. 41-52.

Jenkins, D. & Pearson, F., 1978 . Feasibility of Rainwater Collection Systems in California. *Water Resources Centre, University of California,* p. Contribution No. 173.

Kendall, C. & McDonnell, J. J., 2012. *Isotope tracers in catchment hydrology.* s.l.:Elsevier.

Kitching, R. et al., 1980. Assessment of recharge to aquifers. *Hydrological Sciences Bulletin 25,* p. 217–235.

Kitching, R. & Shearer, T. R., 1982. construction and operation of a large undisturbed lysimeter to measure recharge to the chalk aquifer, England. *Journal of Hydrology 58,* p. 267–277.

Lerner, D. N., Issar, A. S. & Simmers, I., 1990. Groundwater recharge: a guide to understanding and estimating natural recharge, vol. 8. *International Contributions to Hydrogeology*.

Lobo Ferreira, J. P. C., Melo Baptista, J. P., Rodrigues, J. D. & Cunha, L. V., 1981. *http://repositorio.lnec.pt:8080/jspui/handle/123456789/14502.* [Online].

Macedo, C. R., Costa, V. & Ferreira, M., 1974. *K/Ar ages on the central Atlantic islands.* Paris, s.n.

Mandal, B. K. et al., 1998. Impact of safe water for drinking and cooking on five arsenic-affected families for 2 years in West Bengal, India. *Science of total environment, 218,* pp. 185-201.

Manning, B. A. & Goldberg, S., 1997. Adsorption and stability of arsenic (III) at the clay mineral− water interface. *Environmental Science & Technology, 31(7),* pp. 2005-2011.

Mårtensson, E. M. et al., 2003. Laboratory simulations and parameterization of the primary marine aerosol production. *Journal of Geophysical Research: Atmospheres, 108(D9).*

Mata, J. et al., 2013. O arquipelago da Madeira. In: R. Dias, A. Araujo, P. Terrinha & J. C. Kullberg, eds. *Geology of Portugal, Volume II - Meso-Cenozoic Geology of Portugal.* Lisboa: Escolar Editora, pp. 691-746.

Mata, J., Kerrich, R., MacRae, N. D. & Wu, T. W., 1998. Elemental and isotopic (Sr, Nd, and Pb) characteristics of Madeira Island basalts: evidence for a composite HIMU-EM I plume fertilizing lithosphere. *Canadian Journal of Earth Sciences, 35(9),* pp. 980-997.

Mathias, M. D. L., 1988. *An annotated list of the mammals recorded from the Madeira Islands,* Funchal: http://publications.cm-funchal.pt.

Mazor, E. & George, R., 1992. Marine airborne salts applied to trace evaporation, local recharge and lateral groundwater flow in Western Australia. *Journal of Hydrology, 139,* p. 63–77.

McDougall, I. & Schmincke, H. U., 1976. Geochronology of Gran Canaria, Canary Islands: Age of shield building volcanism and other magmatic phases. *Bulletin of Volcanology, Volume 40, Issue 1,* p. 57–77.

McIntosh, J. C. & Walter, L. M., 2006. Paleowater in Silurian-Devonian carbonate aquifers: Geochemical evolution of groundwater in the Great Lakes region since Late Pleistocene. *Geochimica Cosmochimica Acta, 70,* p. 2454–2479.

McLaughlin, D. & Johnson, W. K., 1987. Comparison of three groundwater modeling studies. *Journal of water resources planning and management 113(3),* pp. 405-421.

Meneses, C. A. d., 1914. *Flora do Archipelago da Madeira: (phanerogamicas e cryptogamicas vasculares).* Funchal [Madeira Island]: Junta Agricola da Madeira.

Moller, D., 1990. The Na/Cl ratio in rainwater and the seasalt chloride cycle. *Tellus, 42B,* pp. 254-262.

Moore, J. G. & Clague, D. A., 1992. Volcano growth and evolution of the island of Hawaii. *Geol Soc Am Bull (104),* p. 1471–1484.

Morais, J. C., 1943. *A ilha de Porto Santo e as suas rochas..* Coimbra, Memorias e Noticias, Publ. Mus. Min. Geol. Univ. Coimbra.

Naranjo, G., Cruz-Fuentes, T., Cabrera, M. d. C. & Custodio, E., 2015. Estimating Natural Recharge by Means of Chloride Mass Balance in a Volcanic Aquifer: Northeastern Gran Canaria (Canary Islands, Spain). *Water 7,* pp. 2555-2574.

Naturais, S. R. d. A. e. R., 2016. *Geodiversity itinerary of Porto Santo Island,* Madeira: Regiao Autonoma da Madeira.

Nickson, R. T. et al., 2000. Mechanism of arsenic release to groundwater, Bangladesh and West Bengal. *Applied Geochemistry, 15(4),* pp. 403-413.

Nordstrom, D. K. & Jenne, E. A., 1977. Fluorite solubility equilibria in selected geothermal waters. *Geochimica et Cosmochimica Acta. 41(2),* pp. 175-188.

Penman, H. L., 1948. Natural evaporation from open water, bare soil and grass. *Proceedings of the Royal Society of London, Series A 193*, p. 120–145.

Penman, H. L., 1949. The dependence of transpiration on weather and soil conditions. *Journal of Soil Science 1,* pp. 74-89.

Peters, S. C., Blum, J. D., Klaue, B. & Karagas, M. R., 1999. Arsenic occurrence in New Hampshire drinking water. *Environmental science & technology, 33(9),* pp. 1328-1333.

Philip, J. R., 1980. Field heterogeneity: some basic issues. *Water Resources Research 16(2),* pp. 443-448.

Piper, A. M., 1944. A graphic procedure in the geochemical interpretation of water-analyses. *Eos, Transactions American Geophysical Union, 25(6),* pp. 914-928.

Prada, S. N., da Silva, M. O. & Cruz, J. V., 2005. Groundwater behaviour in Madeira, volcanic island (Portugal). *Hydrogeology Journal, 13,* pp. 800-812.

Prickett, T. A., 1975. Modeling techniques for groundwater evaluations. *Advances in Hydroscience, Volume 10,* pp. 1-143.

Ribeiro, M. L. & Ramalho, M., 2010. *A Geological tour of the archipelago of Madeira,* Lisbon: Direcção Regional do Comércio, Indústria e Energia, Laboratório Nacional de Energia e Geologia, I.P..

Richards, L. A., 1969. *Diagnosis and improvement of saline and alkali soils.* Washington: United States Department Of Agriculture.

Rivera, D. & Obon, C., 1995. The ethnopharmacology of Madeira and Porto Santo Islands, a review. *Journal of Ethnopharmacology,* Volume 46, pp. 73-93.

Robertson, F. N., 1989. Arsenic in ground-water under oxidizing conditions, south-west United States. *Environmental geochemistry and Health, 11(3),* pp. 171-185.

Rushton, K. R. & Ward, C., 1979. The estimation of groundwater recharge. *Journal of Hydrology 41,* p. 345–361.

Saleh, A., Al-Ruwaih, F. & Shehata, M., 1999. Hydrogeochemical processes operating within the main aquifers of Kuwait. *Journal of Arid Environments,* 42(3), pp. 195-209.

Savoie, D. L. & Prospero, J., 1982. Particle size distribution of nitrate and sulfate in the marine atmosphere. *Geophysical Research Letters, 9(10),* pp. 1207-1210.

Saxena, V. & Ahmed, S., 2001. Dissolution of fluoride in groundwater: a water-rock interaction study. *Environmental Geology, 40(9),* pp. 1084-1087.

Schmidt, R., 2000. *From seamount to oceanic island, Porto Santo, Madeira Archipelago (central East-Atlantic). PhD Thesis.* Kiel: Christian Albrechts University Kiel.

Schmidt, R. & Schmincke, H.-U., 2002. From seamount to oceanic island, Porto Santo, central East-Atlantic. *Int J Earth Sci (Geol Rundsch),* p. 91:594–614.

Schmincke, H. U. & Staudigel, H., 1976. *Pillow lavas on central and eastern Atlantic islands (La Palma, Gran Canaria, Porto Santo, Santa Maria).,* s.l.: Bull. Soc. Geol. Fr. 7, 871-883.

Schmincke, H. U. & Weibel, M., 1972. Chemical study of rocks from Madeira, Porto Santo and Sao Miguel, Terceira (Azores). *N. Jb. Miner. Abh., E. Schweizerbart'sche Verlagsbuchhandlung,* Volume 117, pp. 253-281.

Schoeller, H., 1965. Hydrodynamique lans lekarst (ecoulemented emmagusinement). *Actes Colloques Doubronik, I: AIHS et UNESCO,* pp. 3-20.

Schoeller, H., 1967. *Qualitative evaluation of groundwater resources. In Methods and techniques of groundwater investigation and development.* s.l., s.n., p. 44–52.

Schreiber, M. E., Simo, J. A. & Freiberg, P. G., 2000. Stratigraphic and geochemical controls on naturally occurring arsenic in groundwater, eastern Wisconsin, USA. *Hydrogeology Journal, 8(2),* pp. 161-176.

Silva, J. B. P., 2002. *Beach sand of the island of Porto Santo: geology, genesis, dynamics and medicinal properties, Doctoral Dissertation in Geology.* Aveiro: University of Aveiro.

Silva, J. B. P., 2003. *Areia De Praia Da Ilha Do Porto Santo-Geologia, Genese, Dinamica e Propriedades Justificativas do seu Interesse Medicinal.* Madeira: Madeira Rochas.

Silva, J. B. P. et al., 2008. *Estudo hidrogeológico da caracterização e classificação da água subterrânea do Conjunto Turístico Colombo`s Resort, ilha,* Funchal: s.n.

Simpson, H. J. & Herczeg, A. L., 1991. Salinity and evaporation in the river Murray basin, Australia. *Journal of Hydrology, 124(1-2),* pp. 1-27.

Smedley, P. L., Nicolli, H. B., Barros, A. J. & Tullio, J. O., 1998. *Origin and mobility of arsenic in groundwater from the Pampean Plain, Argentina.* Taupo, New Zealand, Balkema, Rotterdam, pp. 275-278.

Soltan, M. E., 1999. Evaluation of groundwater quality in Dakhla Oasis (Egyptian Western Desert). *Environmental Monitoring and Assessment, 57,* p. 157–168.

Thornthwaite, C. W., 1948. An approach toward a rational classification of climate.. *Geographical review, 38(1),* pp. 55-94.

Thornton, I., 1996. Sources and pathways of arsenic in the geochemical environment: health implications. *Geological Society, London, Special Publications, 113(1),* pp. 153-161.

Tossell, J. A., 1997. Theoretical studies on arsenic oxide and hydroxide species in minerals and in aqueous solution. *Geochimica et Cosmochimica Acta, 61(8),* pp. 1613-1623.

Vespermann, D. & Schmincke, H.-U., 1999. Scoria Cones and Tuff Rings. In: *Encyclopedia of Volcanoes.* San Diego: Academic Press, p. 683–694.

Villarreal, E. L. & Dixon, A., 2005. Analysis of a rainwater collection system for domestic water supply in Ringdansen, Norrkoping, Sweden. *Building and Environment, 40,* pp. 1174-1184.

Wallick, E. I. & Tooth, J., 1976. *Methods of regional groundwater flow analysis with suggestions for the use of environmental in groundwater hydrology.* Vienna, s.n., pp. 37-64.

Wang, H. F. & Anderson, M. P., 1990. *Introduction to groundwater modeling: Finite difference and finite element methods.* s.l.:Academic Press.

Weisel, C. P., Duce, R. A., Fasching, J. L. & Heaton, R. W., 1984. Estimates of the transport of trace metals from the ocean to the atmosphere. *Journal of Geophysical Research: Atmospheres, 89(D7),* pp. 11607-11618.

WHO, 2011. Guidelines for drinking-water quality. *WHO chronicle, 38,* pp. 104-8.

Wopfner, H. & Twidale, C. R., 1967. The chemical characteristics of lentic surface waters in Australia. In: *Australian Inland Waters and their Fauna: Eleven Studies.* Canberra: Australian National University Press.

Yan, X. P., Kerrich, R. & Hendry, M. J., 2000. Distribution of arsenic (III), arsenic (V) and total inorganic arsenic in porewaters from a thick till and clay-rich aquitard sequence, Saskatchewan, Canada. *Geochimica et Cosmochimica Acta, 64(15),* pp. 2637-2648.

Yaziz, M., Gunting, H., Sapari, N. & Ghazali, W., 1989. Variations in rainwater quality from roof catchments. *water resources 23 (6),* pp. 761-765.

Appendix A

Table 6 Electrical conductivity of calcarenite and paleosols samples from Porto Santo

		Electrical Conductivity (µS/cm)				
S. No.	**Depth from surface (m)**	**4th Hour**	**8th Hour**	**12th Hour**	**16th Hour**	**20th Hour**
C1	0	321	330	338	335	340
C2	1	3280	3280	3280	3270	3260
C3	4	175	184	194	199	204
C4	4.2	575	589	594	588	606
C5	4.4	139	147	160	163	168
C6	4.6	395	407	414	418	416
C7	4.8	361	364	377	386	386
C8	5	751	760	772	771	776
C9	5.2	388	406	410	411	410
S1	5.25	2000	1962	1921	1921	1974
S2	5.45	1376	1343	1347	1338	1347
S3	5.65	748	731	727	726	741
S4	5.85	842	820	815	815	828
S5	6.05	857	858	851	854	854
S6	6.25	664	653	649	641	658
S7	6.45	475	478	480	472	487
S8	6.65	452	457	459	454	456
S9	6.85	525	529	529	509	509

Appendix B

Table 7 Concentration of major, minor and trace ions in groundwater of Porto Santo

S. No.	pH	EC	Na	K	Ca	Mg	Cl	HCO_3	CO_3	SO_4	NO_3	Br	F	B	Si	As
		µS/cm	mg/L													µg/L
1	8.8	5160	1080	62.1	26.5	25.8	1110	399	12.7	272	39.4	4.0	1.7	4.4	10.4	13.8
2	9.2	5180	1090	79.4	19.1	29.1	1070	368	26.3	288.4	36.2	3.7	1.4	4.5	13.5	24.4
3	7.9	4790	1000	56.5	19.4	39.0	932	603	2.2	248.4	40.3	3.7	2.8	4.1	17.4	12.0
4	8.4	3010	633	14.1	6.1	9.4	530	585	6.9	158.4	42.3	3.3	4.8	1.4	28.1	4.5
5	7.9	6280	1310	65.6	38.5	55.4	1520	586	2.3	264.8	44.3	5.0	3.1	4.4	10.0	12.9
6	7.8	6720	1430	74.3	32.6	62.9	1480	782	2.7	335.2	44.1	5.0	2.8	5.7	16.2	2.2
7	8.5	4780	1090	16.0	9.3	13.6	989	460	6.7	288.4	36.5	3.3	6.0	1.7	13.1	8.8
8	7.9	2280	464	12.9	4.9	8.6	364	462	1.7	171.6	41.3	4.9	4.4	1.0	17.6	0.3
9	8.0	1600	186	11.3	52.6	43.7	412	185	0.9	124	39.9	8.0	2.9	0.3	4.8	2.1
10	7.9	2910	551	34.6	15.5	26.0	561	477	1.9	134	16.5	1.8	1.9	1.0	16.3	1.0
11	7.6	3140	589	18.8	8.1	20.2	739	135	0.3	167.2	37.9	2.9	2.1	1.2	33.3	24.8
12	7.7	5740	845	10.9	47.0	62.6	1460	674	1.7	183.2	43.3	4.3	3.1	1.0	12.1	1.3
13	8.4	3310	689	12.1	12.2	26.5	533	793	10.5	174.8	37.9	1.8	2.9	1.4	18.4	0.6
14	7.9	2770	568	15.2	7.3	10.3	322	535	1.9	91.2	41.9	1.0	2.7	1.6	22.8	1.4
15	7.8	3350	751	19.9	7.3	13.7	540	802	2.7	196	47.8	1.7	3.6	2.3	20.5	1.4
16	7.7	3450	780	34.7	10.7	16.4	536	854	2.0	196	37.7	1.8	4.0	2.3	20.5	1.3
17	8.3	5160	1190	50.0	8.8	21.2	1070	789	7.4	231.2	49.4	3.4	3.3	2.8	13.9	0.0
18	7.6	7330	1700	36.6	28.1	42.7	1690	1211	2.2	381	0.0	5.2	4.9	2.6	31.4	1.5
19	7.8	6070	1160	18.9	62.9	88.4	1670	677	1.9	251	0.0	5.2	2.6	1.4	17.3	0.0
20	7.4	3180	583	19.6	8.8	19.8	788	129	0.2	174	40.3	3.0	1.7	1.6	31.9	25.9
21	8.4	5240	1180	36.3	9.7	20.6	1130	785	9.5	252	92.0	3.8	2.0	3.9	15.2	1.7
22	8.1	1920	186	11.3	52.6	43.7	412	185	0.9	124	0.0	8.0	2.9	0.3	4.8	2.1
23	8.4	3110	648	17.5	9	11.2	566	599	8.1	97.6	14.2	1.8	4.1	2.3	29.6	5.7
24	7.9	5070	1080	33.2	12.3	18.9	1110	883	3.1	199	18.6	3.3	3.5	3.1	20.7	13.4
25	8.2	3920	835	15.4	13.6	22.4	791	617	4.8	165	30.5	2.3	2.2	2.8	28.6	1.7
26	7.9	2300	454	14.8	5.5	8.84	365	464	1.9	88.7	25.2	1.3	3.3	1.5	17.1	0.6
27	6.8	7750	1130	20.4	183	209	2600	442	0.1	383	0.0	7.1	0.0	0.6	34.2	0.0
28	6.9	3680	1150	30.6	98.7	139	2280	250	0.1	374	26.1	6.9	1.0	1.2	32.4	2.8
29	8.5	3160	696	14.2	13.9	25	524	788	13.2	151	8.0	1.5	2.3	2.2	18.6	0.8
30	8.0	6260	1510	39.5	23.4	36	1470	605	2.8	529	38.9	5.2	2.0	4.6	10.2	21.6
31	8.2	4160	1400	39.1	26.1	39.3	1480	548	3.9	508	37.5	5.1	1.8	4.3	10.3	22.5
32	7.8	6720	1430	74.3	32.6	62.9	1600	782	2.7	487	63.3	5.8	2.1	5.7	16.2	2.2
33	7.7	4670	984	33	19	36.6	947	778	1.9	298	65.0	3.2	2.3	3.2	15.3	14.2

S. No.	pH	EC	Na	K	Ca	Mg	Cl	HCO_3	CO_3	SO_4	NO_3	Br	F	B	Si	As
		µS/cm	mg/L													µg/L
34	8.5	4780	1090	16.0	9.3	13.6	1270	460	6.7	385	45.1	4.0	5.9	1.7	13.1	8.8
35	8.5	6380	1260	37.7	29.5	60.4	1740	610	10.4	370	105.3	5.6	2.3	3.8	3.8	16.2
36	7.9	4790	1110	28.9	9.6	18	1040	890	34	239	22.7	3.4	4.4	4.7	15.6	2.8
37	6.7	3373	669	15.7	22.9	34.1	534	741	0.0	161	5.8	1.4	2.9	2.9	26.8	0.5
38	6.7	5300	963	18.1	77.1	102	1200	612	0.0	247	1.3	3.4	3.7	2.5	24.2	0.5
39	6.7	2869	565	19.7	10	21.1	624	161	0.0	157	54.0	2.4	2.3	2.1	46.1	26.0
40	6.6	2429	527	23.9	16.5	25.4	408	484	0.0	130	17.5	1.1	2.4	2.1	23.3	0.6
41	6.7	2077	457	15.5	6.6	9.36	317	430	0.0	88.9	27.2	1.4	4.1	2.0	24.9	0.8
42	6.9	3808	775	26.4	23.5	34	682	595	0.0	198	55.8	2.2	2.9	3.2	33	0.6
43	7.1	4344	868	30	30	42.5	759	674	0.0	227	57.5	2.0	2.4	3.9	35.5	0.5
44	7.6	3055	651	18	9.8	12	515	525	0.0	97.5	12.2	1.4	5.4	2.9	43.4	5.8
45	7.6	5336	1180	30.4	16.9	28	1050	687	52.0	229	9.6	2.9	3.1	4.2	30.2	9.7
46	7.3	1556	174	11.8	52.3	36.3	331	184	0.0	25.9	0.4	1.0	1.5	0.6	6	2.4
47	7.7	5181	1130	31.4	11.3	28.5	916	721	34.0	256	82.3	3.2	3.7	5.8	17.7	1.4
48	7.9	9926	1900	37.2	252	187	2700	514	0.0	480	20.5	8.2	0.4	3.1	42.3	0.4
49	7.5	5402	1270	25.1	25.9	35.1	953	978	0.0	274	1.3	3.2	4.5	4.5	40.7	2.7
50	7.7	1486	340	6.69	6.3	4.53	189	387	0.0	57.6	5.0	0.8	3.3	1.4	29.2	4.4
51	7.4	2011	402	14.7	5.7	9.13	267	404	0.0	104	13.7	0.7	7.9	2.6	17.7	20.9
52	7.9	4139	844	30.6	16.9	33.5	671	633	0.0	232	60.2	2.3	4.2	3.9	23.5	12.9

Appendix C

Table 8 Saturation Index of aragonite, calcite, dolomite, gypsum, halite and quartz

S. No.	Aragonite	Calcite	Dolomite	Gypsum	Halite	Quartz
1	0.8	1.0	2.3	-2.0	-4.6	0.2
2	0.9	1.0	2.6	-2.1	-4.6	0.3
3	0.8	0.9	2.5	-2.4	-4.7	0.5
4	0.0	0.2	0.8	-2.7	-5.1	0.7
5	0.3	0.4	1.2	-1.9	-4.4	0.3
6	0.3	0.4	1.4	-1.9	-4.4	0.5
7	0.1	0.3	1.0	-2.4	-4.6	0.4
8	-0.6	-0.5	-0.4	-2.7	-5.4	0.5
9	0.1	0.3	0.7	-1.8	-5.7	0.0
10	-0.1	0.1	0.7	-2.3	-5.1	0.5
11	-1.2	-1.1	-1.5	-2.5	-5.0	0.8
12	0.3	0.4	1.2	-1.9	-4.6	0.4
13	0.5	0.6	1.9	-2.4	-5.1	0.5
14	-0.4	-0.2	0.0	-2.8	-5.4	0.6
15	-0.3	-0.1	0.3	-2.6	-5.0	0.6
16	-0.3	-0.1	0.3	-2.4	-5.0	0.6
17	0.2	0.3	1.3	-2.5	-4.6	0.4
18	0.1	0.2	0.9	-1.9	-4.2	0.7
19	0.4	0.6	1.6	-1.7	-4.4	0.5
20	-1.4	-1.3	-1.9	-2.5	-5.0	0.8
21	0.3	0.4	1.5	-2.5	-4.5	0.4
22	0.3	0.4	1.1	-1.8	-5.7	-0.1
23	0.3	0.4	1.3	-2.7	-5.1	0.7
24	0.0	0.1	0.7	-2.4	-4.6	0.5
25	0.2	0.4	1.3	-2.4	-4.8	0.7
26	-0.5	-0.3	-0.1	-2.9	-5.4	0.5
27	-0.4	-0.2	-0.1	-1.2	-4.2	0.9
28	-0.7	-0.6	-0.7	-1.4	-4.3	0.7
29	0.7	0.8	2.2	-2.4	-5.1	0.5
30	0.1	0.3	1.1	-1.8	-4.3	0.2
31	0.3	0.5	1.4	-1.8	-4.4	0.2
32	0.2	0.4	1.3	-1.7	-4.3	0.5

S. No.	Aragonite	Calcite	Dolomite	Gypsum	Halite	Quartz
33	-0.1	0.1	0.8	-2.1	-4.7	0.4
34	0.1	0.3	1.0	-2.3	-4.5	0.4
35	0.7	0.9	2.4	-1.9	-4.3	-0.2
36	-0.1	0.0	0.7	-2.5	-4.6	0.4
37	-0.9	-0.8	-1.1	-2.1	-5.1	0.7
38	-0.6	-0.4	-0.5	-1.6	-4.6	0.7
39	-1.9	-1.8	-3.0	-2.4	-5.1	0.9
40	-1.3	-1.2	-1.9	-2.3	-5.3	0.6
41	-1.6	-1.5	-2.5	-2.8	-5.5	0.6
42	-0.9	-0.7	-1.0	-2.1	-4.9	0.8
43	-0.5	-0.4	-0.2	-1.9	-4.8	0.8
44	-0.6	-0.4	-0.4	-2.7	-5.1	0.9
45	-0.3	-0.2	0.2	-2.2	-4.6	0.7
46	-0.5	-0.4	-0.6	-2.4	-5.8	0.1
47	-0.3	-0.2	0.4	-2.3	-4.7	0.5
48	0.9	1.1	2.3	-1.0	-4.0	0.9
49	-0.1	0.0	0.5	-2.0	-4.6	0.9
50	-0.7	-0.5	-0.9	-2.9	-5.8	0.7
51	-1.0	-0.8	-1.2	-2.8	-5.6	0.5
52	0.1	0.2	1.0	-2.2	-4.9	0.6